Author Contributions

Conceived and designed the experiments: NH S.Saitoh MN. Performed the experiments: NH YJ. Analyzed the data: NH. Contributed reagents/materials/analysis tools: NH S.Suzuki. Wrote the paper: NH S.Saitoh MN.

References

1. Vilain E, Le Merrer M, Lecointre C, Desangles F, Kay MA, et al. (1999) IMAGe, a new clinical association of intrauterine growth retardation, metaphyseal dysplasia, adrenal hypoplasia congenita, and genital anomalies. J Clin Endocrinol Metab 84: 4335–4340.
2. Bergadá I, Del Rey G, Lapunzina P, Bergadá C, Fellous M, et al. (2005) Familial occurrence of the IMAGe association: additional clinical variants and a proposed mode of inheritance. J Clin Endocrinol Metab 90: 3186–3190.
3. Hutz JE, Krause AS, Achermann JC, Vilain E, Tauber M, et al. (2006) IMAGe association and congenital adrenal hypoplasia: no disease-causing mutations found in the ACD gene. Mol Genet Metab 88: 66–70.
4. Lienhardt A, Mas JC, Kalifa G, Chaussain JL, Tauber M (2002) IMAGe association: additional clinical features and evidence for recessive autosomal inheritance. Horm Res 57: 71–78.
5. Pedreira CC, Savarirayan R, Zacharin MR (2004) IMAGe syndrome: a complex disorder affecting growth, adrenal and gonadal function, and skeletal development. J Pediatr 144: 274–277.
6. Tan TY, Jameson JL, Campbell PE, Ekert PG, Zacharin M, et al. (2006) Two sisters with IMAGe syndrome: cytomegalic adrenal histopathology, support for autosomal recessive inheritance and literature review. Am J Med Genet A 140: 1778–1784.
7. Amano N, Hori N, Ishii T, Narumi S, Hachiya R, et al. (2008) Radiological evolution in IMAGe association: a case report. Am J Med Genet A 146A: 2130–2133.
8. Balasubramanian M, Sprigg A, Johnson DS (2010) IMAGe syndrome: Case report with a previously unreported feature and review of published literature. Am J Med Genet A 152A: 3138–3142.
9. Arboleda VA, Lee H, Parnaik R, Fleming A, Banerjee A, et al. (2012) Mutations in the PCNA-binding domain of CDKN1C cause IMAGe syndrome. Nat Genet 44: 788–792.
10. Lee MH, Reynisdóttir I, Massagué J (1995) Cloning of p57KIP2, a cyclin-dependent kinase inhibitor with unique domain structure and tissue distribution. Genes Dev 9: 639–649.
11. Pateras IS, Apostolopoulou K, Niforou K, Kotsinas A, Gorgoulis VG (2009) p57KIP2: "Kip"ing the cell under control. Mol Cancer Res 7: 1902–1919.
12. Hatada I, Ohashi H, Fukushima Y, Kaneko Y, Inoue M, et al. (1996) An imprinted gene p57KIP2 is mutated in Beckwith-Wiedemann syndrome. Nat Genet 14: 171–173.
13. Touitou R, Richardson J, Bose S, Nakanishi M, Rivett J, et al. (2001) A degradation signal located in the C-terminus of p21WAF1/CIP1 is a binding site for the C8 alpha-subunit of the 20S proteasome. EMBO J 15: 2367–2375.
14. Yan Y, Frisén J, Lee MH, Massagué J, Barbacid M (1997) Ablation of the CDK inhibitor p57Kip2 results in increased apoptosis and delayed differentiation during mouse development. Genes Dev 11: 973–983.
15. Zhang P, Liégeois NJ, Wong C, Finegold M, Hou H, et al. (1997) Altered cell differentiation and proliferation in mice lacking p57KIP2 indicates a role in Beckwith-Wiedemann syndrome. Nature 387: 151–158.
16. Takahashi K, Nakayama K, Nakayama K (2000) Mice lacking a CDK inhibitor, p57Kip2, exhibit skeletal abnormalities and growth retardation. J Biochem 127: 73–83.
17. Nakanishi M, Robetorye RS, Pereira-Smith OM, Smith JR (1995) The C-terminal region of p21SDI1/WAF1/CIP1 is involved in proliferating cell nuclear antigen binding but does not appear to be required for growth inhibition. J Biol Chem 270: 17060–17063.
18. Watanabe H, Pan ZQ, Schreiber-Agus N, DePinho RA, Hurwitz J, et al. (1998) Suppression of cell transformation by the cyclin-dependent kinase inhibitor p57KIP2 requires binding to proliferating cell nuclear antigen. Proc Natl Acad Sci U S A. 95: 1392–1397.
19. Lu Z, Hunter T (2010) Ubiquitylation and proteasomal degradation of the p21Cip1, p27Kip1 and p57Kip2 CDK inhibitors. Cell Cycle 9: 2342–2352.
20. Sarostina NG, Kipreos ET (2012) Multiple degradation pathways regulate versatile CIP/KIP CDK inhibitors. Trends Cell Biol 22: 33–41.
21. Kamura T, Hara T, Kotoshiba S, Yada M, Ishida N, et al. (2003) Degradation of p57Kip2 mediated by SCFSkp2-dependent ubiquitylation. Proc Natl Acad Sci 100: 10231–10236.
22. Kim M, Nakamoto T, Nishimori S, Tanaka K, Chiba T (2008) A new ubiquitin ligase involved in p57KIP2 proteolysis regulates osteoblast cell differentiation. EMBO Rep 9: 878–884.
23. Jin Y, Lee H, Zeng SX, Dai MS, Lu H (2003) MDM2 promotes p21waf1/clip1 proteasomal turnover independently of ubiquitylation. EMBO J 23: 6365–6377.
24. Jin Y, Zeng SX, Sun XX, Lee H, Blattner C, et al. (2008) MDMX promotes proteosomal turnover of p21at G1 and early S phases independently of, but in cooperation with, MDM2. Mol Cell Biol 28: 1218–1229.
25. Wang B, Liu K, LinHY, Bellam N, Ling S, et al. (2010) 14-3-3 Tau regulates ubiquitin-independent proteasomal degradation of p21, a novel mechanism of p21 downregulation in breast cancer. Mol Cell Biol 30: 1508–27.

Biochemical and Biophysical Research Communications xxx (2014) xxx–xxx

Contents lists available at ScienceDirect

Biochemical and Biophysical Research Communications

journal homepage: www.elsevier.com/locate/ybbrc

The processed isoform of the translation termination factor eRF3 localizes to the nucleus to interact with the ARF tumor suppressor

Yoshinori Hashimoto, Naoyuki Kumagai, Nao Hosoda, Shin-ichi Hoshino *

Department of Biological Chemistry, Graduate School of Pharmaceutical Sciences, Nagoya City University, Nagoya 467-8603, Japan

ARTICLE INFO

Article history:
Received 12 February 2014
Available online xxxx

Keywords:
Translation termination
eRF3
IAP
Apoptosis
NES
ARF

ABSTRACT

The eukaryotic releasing factor eRF3 is a multifunctional protein that plays pivotal roles in translation termination as well as the initiation of mRNA decay. eRF3 also functions in the regulation of apoptosis; eRF3 is cleaved at Ala73 by an as yet unidentified protease into processed isoform of eRF3 (p-eRF3), which interacts with the inhibitors of apoptosis proteins (IAPs). The binding of p-eRF3 with IAPs leads to the release of active caspases from IAPs, which promotes apoptosis. Although full-length eRF3 is localized exclusively in the cytoplasm, p-eRF3 localizes in the nucleus as well as the cytoplasm. We here focused on the role of p-eRF3 in the nucleus. We identified leptomycin-sensitive nuclear export signal (NES) at amino acid residues 61–71 immediately upstream of the cleavage site Ala73. Thus, the proteolytic cleavage of eRF3 into p-eRF3 leads to release an amino-terminal fragment containing NES to allow the relocalization of eRF3 into the nucleus. Consistent with this, p-eRF3 more strongly interacted with the nuclear ARF tumor suppressor than full-length eRF3. These results suggest that while p-eRF3 interacts with IAPs to promote apoptosis in the cytoplasm, p-eRF3 also has some roles in regulating cell death in the nucleus.

1. Introduction

eRF3 is an evolutionarily conserved polypeptide chain releasing factor that functions in translation termination and termination-coupled events. The yeast eRF3 gene Gst1 was initially identified as essential gene for G1-to-S phase transition in the cell cycle [1]. The gene was also cloned as the omnipotent suppressor *SUP35* [2]. Two eRF3 genes, GSPT1 and GSPT2, have been identified to date in mammals [3,4], the products of which were later renamed as eRF3a and eRF3b, respectively [5]. eRF3 consists of two regions, an amino-terminal unstructured domain (N-domain) and translation elongation factor eEF1A-like GTP-binding domain (C-domain). The role of eRF3 is well-established in translation termination, in which eRF3 interacts with another releasing factor, eRF1 in its C-domain to accelerate the polypeptide chain releasing reaction catalyzed by the ribosome [6–9].

On the other hand, the N-domain of eRF3 is not necessary for the termination reaction, but interacts with the poly(A)-binding protein PABP to play a pivotal role in the initiation of mRNA decay [10]. eRF3, via an interaction with PABP, also functions in the translation cycle by efficiently recycling the terminating ribosome to the initiation complex [11]. Furthermore, eRF3 was shown to be involved in the initiation of nonsense-mediated mRNA decay (NMD), which rapidly degrades aberrant mRNAs containing premature termination codons [12]. Thus, eRF3 is a multifunctional regulator of gene expression.

The proteolytically processed isoform of eRF3 (p-eRF3) acts as a regulator of apoptosis. eRF3 has been shown to be cleaved at the 73A residue by an unknown protease, leading to the exposure of a conserved inhibitor of apoptosis protein (IAP)-binding motif (IBM) at its N-terminus [13]. Smac/DIABLO and Omi/HtrA2 are IBM-containing proteins that have been extensively examined in humans. Both proteins are localized in the intermembrane space of mitochondria and are released into the cytosol during apoptosis to interact with IAPs, which leads to the activation of caspase due to their liberation from IAP inhibition [14–20]. In a similar manner, the N-terminally processed p-eRF3 also promotes apoptosis by binding with IAPs [13]. This study defined eRF3 as a novel regulator of cell death. The above-described functions of eRF3 are thought to occur in the cytoplasm; however, this study suggested that p-eRF3 may also function in the nucleus; p-eRF3 is localized not only in

Abbreviations: IAP, inhibitor of apoptosis protein; NES, nuclear export signal; NLS, nuclear localization signal; ORF, open reading frame.

* Corresponding author. Fax: +81 52 836 3427.
E-mail address: hoshino@phar.nagoya-cu.ac.jp (S.-i. Hoshino).

http://dx.doi.org/10.1016/j.bbrc.2014.02.063
0006-291X/© 2014 Published by Elsevier Inc.

the cytoplasm, but also in the nucleus, whereas full-length eRF3 is localized exclusively in the cytoplasm. This prompted us to investigate the mechanism responsible for the nucleocytoplasmic shuttling of eRF3 and the role of p-eRF3 in the nucleus. In the present study, we demonstrate that the amino acid sequence (60–71) of eRF3, which is localized immediately upstream of the cleavage site, acts as a functional NES, and the removal of NES by an unknown protease allows p-eRF3 to localize in the nucleus and interact with the nuclear tumor suppressor ARF, which is known to inhibit cell growth in a p53-dependent or -independent manner [21]. The role of p-eRF3 in the nucleus has been discussed herein.

2. Materials and methods

2.1. Cell culture and transfection

HeLa cells were cultured in Dulbecco's modified Eagle's medium (Nissui) supplemented with 5% fetal bovine serum (Sigma) and maintained at 37 °C in 5% CO_2. NIH3T3 cells were cultured in DMEM supplemented with 10% fetal bovine serum (Sigma). HeLa cells were transfected with plasmid using Polyethyleneimine MAX (Polysciences). NIH3T3 cells were transfected with plasmids using LipofectAMINE 2000 (Invitrogen).

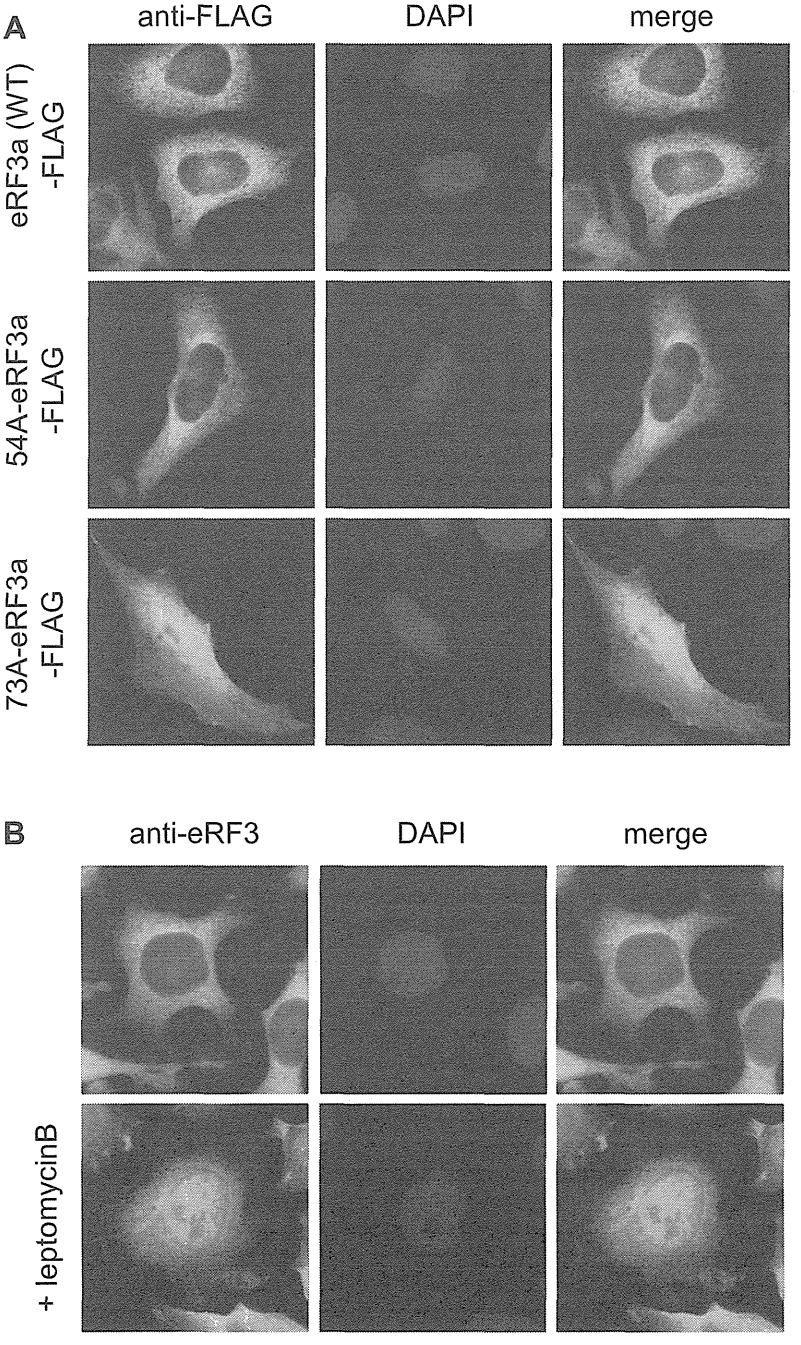

Fig. 1. p-eRF3 localizes in the nucleus as well as the cytoplasm, and is exported from the nucleus in a CRM1-dependent manner. (A) HeLa cells were transfected with pCMV-MycFLAG-Ub-hGSPT1, pCMV-MycFLAG-Ub-(54A)-hGSPT1, and pCMV-MycFLAG-Ub-(73A)-hGSPT1 expressing Ub-(wt)-eRF3a-FLAG, Ub-(54A)-eRF3a-FLAG, and Ub-(73A)-eRF3a-FLAG proteins, respectively, and cells were stained using an anti-FLAG antibody combined with anti-mouse Alexa 488. Nuclei were stained with DAPI. The localization of the FLAG-tagged eRF3 was observed using fluorescence microscopy. (B) HeLa cells treated with or without leptomycin B for 4 h were stained by an anti-eRF3 antibody combined with anti-rabbit Alexa 488. Nuclei were stained with DAPI. The localization of endogenous eRF3 was observed using fluorescence microscopy.

Please cite this article in press as: Y. Hashimoto et al., The processed isoform of the translation termination factor eRF3 localizes to the nucleus to interact with the ARF tumor suppressor, Biochem. Biophys. Res. Commun. (2014), http://dx.doi.org/10.1016/j.bbrc.2014.02.063

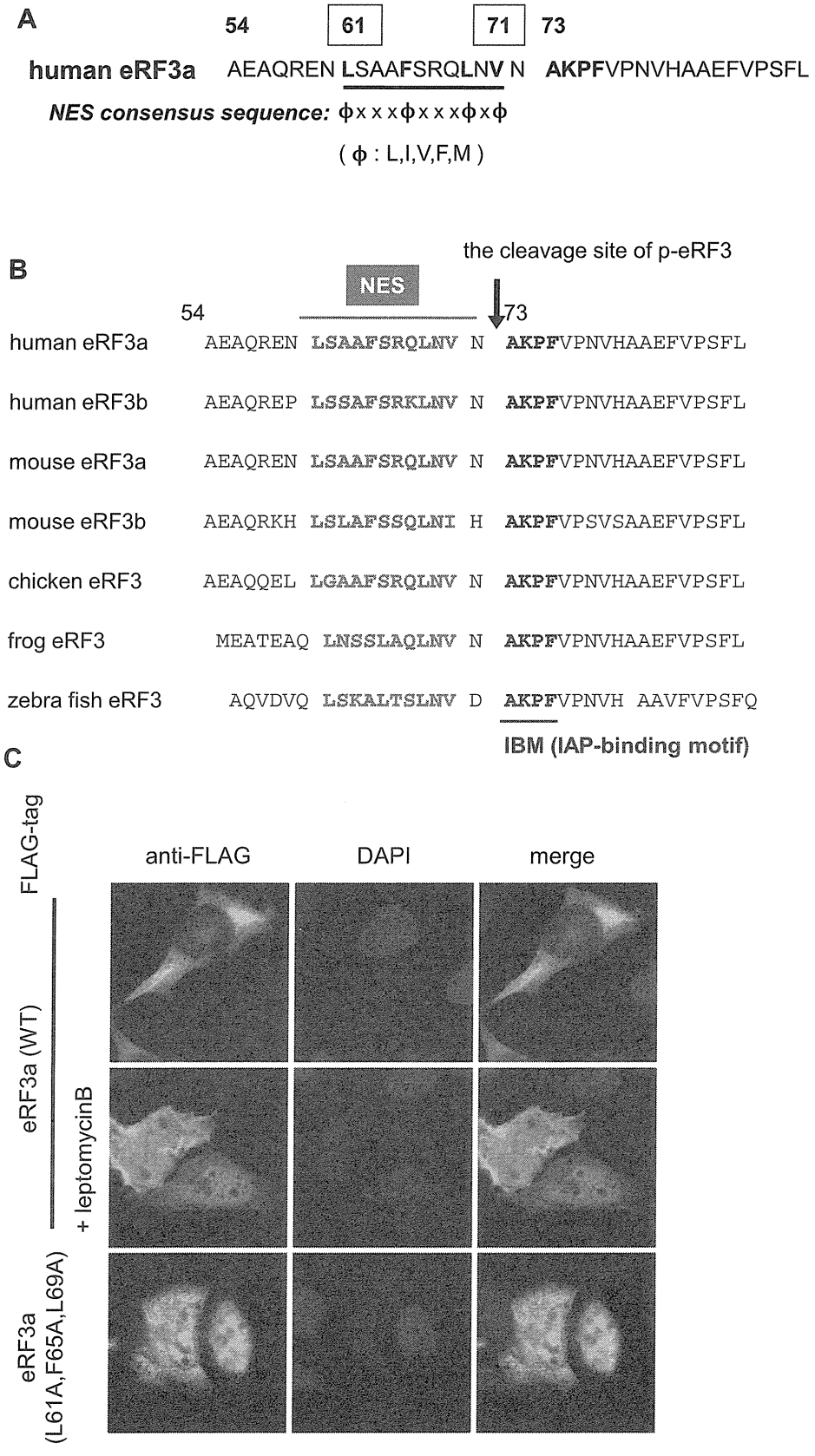

Fig. 2. Identification of the nuclear export signal (NES) motif in eRF3. (A) The leptomycin-sensitive nuclear export signal (NES) in human eRF3a was identified at amino acid residues 61–71 immediately upstream of the cleavage site Ala73. (B) The alignment of amino acid sequences around NES and the cleavage site of p-eRF3. The amino acid sequences of human eRF3a, human eRF3b, mouse eRF3a, mouse eRF3b, chicken eRF3, frog eRF3, and zebra fish eRF3 are shown. (C) HeLa cells were transfected with pFLAG-CMV2-hGSPT1 and pFLAG-CMV2-hGSPT1 (L61A,F65A,L69A), expressing FLAG-eRF3a and FLAG-eRF3a (L61A,F65A,L69A), respectively, and the cells were stained by an anti-FLAG antibody combined with anti-mouse Alexa 488. Nuclei were stained with DAPI. The localization of FLAG-tagged eRF3a was observed using fluorescence microscopy. HeLa cells expressing FLAG-eRF3a, which were treated with leptomycin B, were also shown (+leptomycin B).

Please cite this article in press as: Y. Hashimoto et al., The processed isoform of the translation termination factor eRF3 localizes to the nucleus to interact with the ARF tumor suppressor, Biochem. Biophys. Res. Commun. (2014), http://dx.doi.org/10.1016/j.bbrc.2014.02.063

2.2. Plasmid

To construct pFLAG-CMV2-hGSPT1 (L61A,F65A,L69A), the corresponding region of hGSPT1 cDNA was amplified by inverse PCR using primer pairs NH149 (5′-AAC GTC AAC GCC AAG CCC TTC-3′)/NH150 (5′-GGC TTG CCG GCT GGC GGC CGC GCT GGC GTT CTC CCG CTG-3′), and pFLAG-CMV2-hGSPT1 [4] as a template. To construct pCMV-5xMyc-p14ARF, ORF of p14ARF was amplified by PCR using primer pairs NH174 (5′-GGC GAA TTC ATG GTG CGC AGG TTC TTG G-3′)/NH175 (5′-TCC TCA GCC AGG TCC ACG GGC-3′), and random primer cDNA library obtained from HeLa cells as a template. The resulting cDNA fragment was digested with EcoRI and inserted into the EcoRI and EcoRV sites of pCMV-5xMyc [22].

2.3. Immunostaining

HeLa cells grown on cover glass were fixed by 4% paraformaldehyde (PFA) in PBS(-) for 15 min. After washing 2 times with PBS(-) containing 10 mM glycine, the cells were permeabilized by PBS(-) containing 1% goat serum and 0.1% Triton X-100 for 15 min. The cells were then washed once with PBS(-) and incubated with an anti-FLAG antibody (Sigma) (1/400 dilution) or anti-eRF3 antibody [23] in PBS(-) containing 1% goat serum in a moisture box overnight. After washing 3 times with PBS(-), cells were incubated with Alexa 488 (Invitrogen) (1/400) and 4′, 6-diamidino-2-phenylindole (DAPI) (Dojindo) (1/1000) in PBS(-) containing 1% goat serum for 90 min, and were then washed 3 times with PBS(-). The cover glass was mounted on a glass slide using Prolong Gold (Invitrogen).

2.4. Immunoprecipitation

NIH3T3 cells were lysed in buffer A (20 mM Tris–HCl (pH 7.5), 150 mM NaCl, 0.5% NP-40, 1 mM EDTA, 1 mM dithiothreitol, 0.1 mM PMSF, 2 μg/ml aprotinin, 2 μg/ml leupeptin, and 2 μg/ml pepstatin A) and cells were placed on ice for 15 min after sonication (10 pulses). The supernatant was prepared by centrifugation at 15,000 rpm for 15 min at 4 °C and incubated with anti-Flag IgG agarose (Sigma) for 30 min in the cold room. The resin was washed three times with buffer A. Bound protein was eluted with SDS–PAGE sample buffer and analyzed by Western blotting.

3. Results

3.1. Removal of the amino acid residues (54–72) of eRF3 is responsible for the nuclear localization of p-eRF3

A previous study demonstrated that p-eRF3 interacted with IAPs to promote apoptosis [13]. This study also reported that while full-length eRF3 localized exclusively in the cytoplasm and associated with ER, p-eRF3 was released from the ER and localized both in the cytoplasm and nucleus. These results suggest that eRF3 may be a nucleocytoplasmic shuttling protein. Thus, we attempted to elucidate the mechanism responsible for regulating the subcellular localization of eRF3/p-eRF3. Because p-eRF3 is generated by proteolytic cleavage at Ala73, we hypothesized that the N-terminal region (1–72) released from eRF3 may contain a signal that defines cytoplasmic localization. To examine this possibility, we analyzed the subcellular localization of the N-terminal deletion mutants of eRF3. HeLa cells were transfected with plasmids expressing ubiquitin (Ub)-tagged eRF3a-fusion proteins, in which ubiquitin was fused with eRF3a deletion mutants [23]. According to the Ub fusion protein approach, the Ub moiety of the expressed fusion proteins is cleaved by multiple ATP-dependent proteases, and eRF3a fragments without Ub can be produced [13]. We confirmed that p-eRF3 (73A-eRF3) localized both in the cytoplasm and nucleus, whereas full-length eRF3 localized exclusively in the cytoplasm (Fig. 1A). As we already demonstrated in our previous study that the caspase-cleaved form of eRF3 (33Q-eRF3) localized in the cytoplasm [23], we examined 54A-eRF3 to further narrow the region of eRF3 required for its cytoplasmic localization. 54A-eRF3 exhibited cytoplasmic localization (Fig. 1A). These results indicate that the 19-amino-acid region (54–72) contains a signal that defines the cytoplasmic localization of eRF3.

3.2. eRF3 is exported from the nucleus in a CRM1-dependent manner

Since the CRM1-dependent nuclear export system has already established in detail, we next examined the effects of Leptomycin B, a specific inhibitor of CRM1, on the subcellular localization of eRF3. As shown in Fig. 1B, eRF3 localized not only in the cytoplasm, but also in the nucleus following the Leptomycin B treatment, which indicates that eRF3 is a nucleocytoplasmic shuttling protein that is exported from the nucleus in a manner dependent on CRM1.

3.3. Identification of a functional nuclear export signal (NES) in eRF3

The above results identified eRF3 as a dynamic protein, the cellular localization of which was regulated through the CRM1-dependent nuclear export pathway and the 19-amino-acid region (54–72) contained a cytoplasmic localization signal. We noticed a stretch of hydrophobic residues with a characteristic spacing that resembled leucine-rich NES in the 19-amino-acid region (54–72) (Fig. 2A) [24]. This sequence was highly conserved from zebra fish to humans (Fig. 2B). To confirm that the NES-like sequence identified in eRF3a acts as a functional NES, we introduced alanine mutations into the consensus hydrophobic residues (61LSAAFSRQL NV71). eRF3a (L61A/F65A/L69A) localized both in the cytoplasm and nucleus, as observed for wild type eRF3a in cells treated with LMB (Fig. 2C). We also obtained similar results by using GFP-fused eRF3a (data not shown). These results indicate that 61LSAAFSR QLNV71 of eRF3a is a functional NES. Moreover, p-eRF3 that fused with the amino acid sequence (60–71) of eRF3a at its C-terminus again re-localized exclusively in the cytoplasm, which further supported our conclusion (data not shown). Thus, the proteolytic cleavage of eRF3 by an unknown protease leads to the removal of the NES located immediately upstream of the cleavage site to produce p-eRF3, which in turn allows p-eRF3 to localize in the nucleus as well as the cytoplasm.

3.4. p-eRF3 interacts with p14ARF

To gain further insight into the role of nuclear translocated p-eRF3, we next examined the interaction between p-eRF3 and the

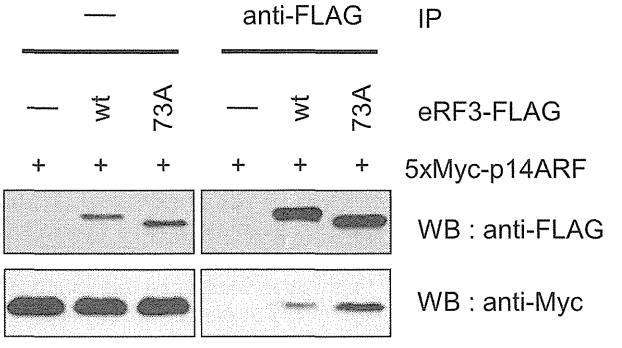

Fig. 3. p-eRF3 interacts with the ARF tumor suppressor in living cells. NIH3T3 cells were transfected with pCMV-5xMyc-p14ARF and either pCMV-MycFLAG, pCMV-MycFLAG-Ub-hGSPT1/eRF3a or pCMV-MycFLAG-Ub-(73A)-hGSPT1/eRF3a. Whole cell extracts were immunoprecipitated (IP) using an anti-FLAG antibody. The immunoprecipitates and inputs were analyzed by Western blotting using anti-FLAG and anti-Myc antibodies.

Please cite this article in press as: Y. Hashimoto et al., The processed isoform of the translation termination factor eRF3 localizes to the nucleus to interact with the ARF tumor suppressor, Biochem. Biophys. Res. Commun. (2014), http://dx.doi.org/10.1016/j.bbrc.2014.02.063

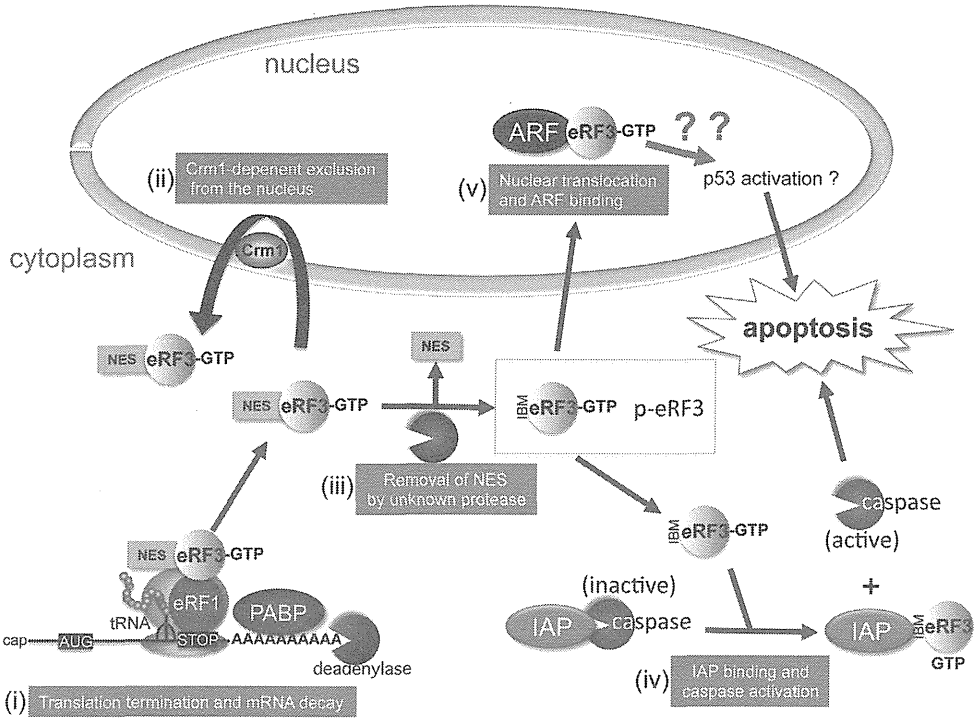

Fig. 4. A hypothetical model describing the possible role of nucleocytoplasmic shuttling of eRF3. (i) In the cytoplasm, eRF3 binds with eRF1 to regulate the termination of translation and termination-coupled initiation of mRNA decay. (ii) NES located immediately upstream of the IAP-binding motif (IBM) of eRF3 acts as a signal to exclude eRF3 from the nucleus. (iii) The removal of NES by an unknown protease produces p-eRF3, which exposes IBM at the N-terminus. (iv) The binding of p-eRF3 IBM with IAPs disrupts their interaction with the initiator caspase-9 and effector caspases-3 and -7, which allows the activation of caspases. (v) The removal of NES allows the nuclear translocation of p-eRF3 and its interaction with the nuclear tumor suppressor ARF.

tumor suppressor p14ARF. A previous study identified p14ARF as a binding partner of eRF3 by yeast two-hybrid screening. eRF3 was shown to bind to p14ARF in an *in vitro* binding assay [25]. However, the interaction between full-length eRF3 and p14ARF was not demonstrated in living cells because eRF3 was localized exclusively in the cytoplasm, whereas p14ARF was in the nucleus. Thus, we expressed 5xMyc-tagged p14ARF and either Flag-eRF3a or Flag-p-eRF3a (73A-eRF3) in NIH3T3 cells, and performed immunoprecipitation experiments with the anti-Flag antibody. As shown in Fig. 3, p-eRF3a (73A-eRF3a) bound more strongly with p14ARF than full-length eRF3a (see Fig. 4).

4. Discussion

A previous study demonstrated that eRF3 is proteolytically processed into an IAP-binding protein to promote apoptosis [13]. The binding of p-eRF3 with IAPs disrupts their interaction with the initiator caspase-9 and effector caspases-3 and -7, which allows the activation of caspases. In the present study, we have newly demonstrated the following: (i) eRF3 is a nucleocytoplasmic shuttling protein and is exported from the nucleus in a manner dependent on CRM1; (ii) 61LSAAFSRQLNV71 located immediately upstream of the proteolytic cleavage site of eRF3 acts as a functional NES; (iii) the removal of NES allows p-eRF3 to localize to the nucleus as well as cytoplasm; (iv) p-eRF3 more strongly interacts with the nuclear ARF tumor suppressor than full-length eRF3. Thus, the proteolytic cleavage of eRF3 at Ala73 leads to the removal of NES located immediately upstream of the cleavage site to produce p-eRF3, which in turn allows p-eRF3 to translocate to the nucleus and interact with p14ARF. p14ARF is best known for its induction of p53-dependent cell death or growth arrest; p14ARF binds to inactivate Mdm2, an E3 ubiquitin ligase for p53, and stabilize p53 to stimulate the transcriptional activity of p53. Therefore, besides promoting apoptosis by binding to IAPs, p-eRF3 may translocate to the nucleus to further promote apoptosis through the p14ARF-p53 pathway. This possibility is now under investigation in our laboratory.

Conflict of interest

The authors declare that they have no conflict of interest.

Acknowledgments

This work was supported by a Grant-in-Aid for Scientific Research on Innovative Areas "RNA regulation" (No. 20112005) from the Ministry of Education, Culture, Sports, Science and Technology of Japan, and a Grant-in-Aid for Scientific Research (B) (No. 21370080) from Japan Society for the Promotion of Science (to S.H.).

References

[1] Y. Kikuchi, H. Shimatake, A. Kikuchi, A yeast gene required for the G1-to-S transition encodes a protein containing an A-kinase target site and GTPase domain, EMBO J. 7 (1988) 1175–1182.
[2] V.V. Kushnirov, M.D. Ter-Avanesyan, M.V. Telckov, A.P. Surguchov, V.N. Smirnov, S.G. Inge-Vechtomov, Nucleotide sequence of the SUP2 (SUP35) gene of *Saccharomyces cerevisiae*, Gene 66 (1988) 45–54.
[3] S. Hoshino, H. Miyazawa, T. Enomoto, F. Hanaoka, Y. Kikuchi, A. Kikuchi, M. Ui, A human homologue of the yeast GST1 gene codes for a GTP-binding protein and is expressed in a proliferation-dependent manner in mammalian cells, EMBO J. 8 (1989) 3807–3814.
[4] S. Hoshino, M. Imai, M. Mizutani, Y. Kikuchi, F. Hanaoka, M. Ui, T. Katada, Molecular cloning of a novel member of the eukaryotic polypeptide chain-releasing factors (eRF). Its identification as eRF3 interacting with eRF1, J. Biol. Chem. 273 (1998) 22254–22259.
[5] C.G. Jakobsen, T.M. Segaard, O. Jean-Jean, L. Frolova, J. Justesen, Identification of a novel termination release factor eRF3b expressing the eRF3 activity in vitro and in vivo, Mol. Biol. (Mosk) 35 (2001) 672–681.

Please cite this article in press as: Y. Hashimoto et al., The processed isoform of the translation termination factor eRF3 localizes to the nucleus to interact with the ARF tumor suppressor, Biochem. Biophys. Res. Commun. (2014), http://dx.doi.org/10.1016/j.bbrc.2014.02.063

[6] G. Zhouravleva, L. Frolova, X. Le Goff, R. Le Guellec, S. Inge-Vechtomov, L. Kisselev, M. Philippe, Termination of translation in eukaryotes is governed by two interacting polypeptide chain release factors, eRF1 and eRF3, EMBO J. 14 (1995) 4065–4072.

[7] L. Frolova, X. Le Goff, G. Zhouravleva, E. Davydova, M. Philippe, L. Kisselev, Eukaryotic polypeptide chain release factor eRF3 is an eRF1- and ribosome-dependent guanosine triphosphatase, RNA 2 (1996) 334–341.

[8] E.Z. Alkalaeva, A.V. Pisarev, L.Y. Frolova, L.L. Kisselev, T.V. Pestova, In vitro reconstitution of eukaryotic translation reveals cooperativity between release factors eRF1 and eRF3, Cell 125 (2006) 1125–1136.

[9] J. Salas-Marco, D.M. Bedwell, GTP hydrolysis by eRF3 facilitates stop codon decoding during eukaryotic translation termination, Mol. Cell. Biol. 24 (2004) 7769–7778.

[10] Y. Funakoshi, Y. Doi, N. Hosoda, N. Uchida, M. Osawa, I. Shimada, M. Tsujimoto, T. Suzuki, T. Katada, S. Hoshino, Mechanism of mRNA deadenylation: evidence for a molecular interplay between translation termination factor eRF3 and mRNA deadenylases, Genes Dev. 21 (2007) 3135–3148.

[11] N. Uchida, S. Hoshino, H. Imataka, N. Sonenberg, T. Katada, A novel role of the mammalian GSPT/eRF3 associating with poly(A)-binding protein in Cap/Poly(A)-dependent translation, J. Biol. Chem. 277 (2002) 50286–50292.

[12] I. Kashima, A. Yamashita, N. Izumi, N. Kataoka, R. Morishita, S. Hoshino, M. Ohno, G. Dreyfuss, S. Ohno, Binding of a novel SMG-1-Upf1-eRF1-eRF3 complex (SURF) to the exon junction complex triggers Upf1 phosphorylation and nonsense-mediated mRNA decay, Genes Dev. 20 (2006) 355–367.

[13] R. Hegde, S.M. Srinivasula, P. Datta, M. Madesh, R. Wassell, Z. Zhang, N. Cheong, J. Nejmeh, T. Fernandes-Alnemri, S. Hoshino, E.S. Alnemri, The polypeptide chain-releasing factor GSPT1/eRF3 is proteolytically processed into an IAP-binding protein, J. Biol. Chem. 278 (2003) 38699–38706.

[14] C. Du, M. Fang, Y. Li, L. Li, X. Wang, Smac, a mitochondrial protein that promotes cytochrome c-dependent caspase activation by eliminating IAP inhibition, Cell 102 (2000) 33–42.

[15] A.M. Verhagen, P.G. Ekert, M. Pakusch, J. Silke, L.M. Connolly, G.E. Reid, R.L. Moritz, R.J. Simpson, D.L. Vaux, Identification of DIABLO, a mammalian protein that promotes apoptosis by binding to and antagonizing IAP proteins, Cell 102 (2000) 43–53.

[16] Y. Suzuki, Y. Imai, H. Nakayama, K. Takahashi, K. Takio, R. Takahashi, A serine protease, HtrA2, is released from the mitochondria and interacts with XIAP, inducing cell death, Mol. Cell 8 (2001) 613–621.

[17] R. Hegde, S.M. Srinivasula, Z. Zhang, R. Wassell, R. Mukattash, L. Cilenti, G. DuBois, Y. Lazebnik, A.S. Zervos, T. Fernandes-Alnemri, E.S. Alnemri, Identification of Omi/HtrA2 as a mitochondrial apoptotic serine protease that disrupts inhibitor of apoptosis protein-caspase interaction, J. Biol. Chem. 277 (2002) 432–438.

[18] A.M. Verhagen, J. Silke, P.G. Ekert, M. Pakusch, H. Kaufmann, L.M. Connolly, C.L. Day, A. Tikoo, R. Burke, C. Wrobel, R.L. Moritz, R.J. Simpson, D.L. Vaux, HtrA2 promotes cell death through its serine protease activity and its ability to antagonize inhibitor of apoptosis proteins, J. Biol. Chem. 277 (2002) 445–454.

[19] L.M. Martins, I. Iaccarino, T. Tenev, S. Gschmeissner, N.F. Totty, N.R. Lemoine, J. Savopoulos, C.W. Gray, C.L. Creasy, C. Dingwall, J. Downward, The serine protease Omi/HtrA2 regulates apoptosis by binding XIAP through a reaper-like motif, J. Biol. Chem. 277 (2002) 439–444.

[20] G. van Loo, M. van Gurp, B. Depuydt, S.M. Srinivasula, I. Rodriguez, E.S. Alnemri, K. Gevaert, J. Vandekerckhove, W. Declercq, P. Vandenabeele, The serine protease Omi/HtrA2 is released from mitochondria during apoptosis. Omi interacts with caspase-inhibitor XIAP and induces enhanced caspase activity, Cell Death Differ. 9 (2002) 20–26.

[21] C.J. Sherr, Divorcing ARF and p53: an unsettled case, Nat. Rev. Cancer 6 (2006) 663–673.

[22] N. Hosoda, Y. Funakoshi, M. Hirasawa, R. Yamagishi, Y. Asano, R. Miyagawa, K. Ogami, M. Tsujimoto, S. Hoshino, Anti-proliferative protein Tob negatively regulates CPEB3 target by recruiting Caf1 deadenylase, EMBO J. 30 (2011) 1311–1323.

[23] Y. Hashimoto, N. Hosoda, P. Datta, E.S. Alnemri, S. Hoshino, Translation termination factor eRF3 is targeted for caspase-mediated proteolytic cleavage and degradation during DNA damage-induced apoptosis, Apoptosis 17 (2012) 1287–1299.

[24] T. la Cour, L. Kiemer, A. Mølgaard, R. Gupta, K. Skriver, S. Brunak, Analysis and prediction of leucine-rich nuclear export signals, Protein Eng. Des. Sel. 17 (2004) 527–536.

[25] V. Tompkins, J. Hagen, V.P. Zediak, D.E. Quelle, Identification of novel ARF binding proteins by two-hybrid screening, Cell Cycle 5 (2006) 641–646.

Please cite this article in press as: Y. Hashimoto et al., The processed isoform of the translation termination factor eRF3 localizes to the nucleus to interact with the ARF tumor suppressor, Biochem. Biophys. Res. Commun. (2014), http://dx.doi.org/10.1016/j.bbrc.2014.02.063

Oncogene (2014) **33,** 55–64

www.nature.com/onc

ORIGINAL ARTICLE

Antiproliferative protein Tob directly regulates c-myc proto-oncogene expression through cytoplasmic polyadenylation element-binding protein CPEB

K Ogami, N Hosoda, Y Funakoshi and S Hoshino

The regulation of mRNA deadenylation constitutes a pivotal mechanism of the post-transcriptional control of gene expression. Here we show that the antiproliferative protein Tob, a component of the Caf1–Ccr4 deadenylase complex, is involved in regulating the expression of the proto-oncogene c-myc. The c-myc mRNA contains *cis* elements (CPEs) in its 3′-untranslated region (3′-UTR), which are recognized by the cytoplasmic polyadenylation element-binding protein (CPEB). CPEB recruits Caf1 deadenylase through interaction with Tob to form a ternary complex, CPEB–Tob–Caf1, and negatively regulates the expression of c-myc by accelerating the deadenylation and decay of its mRNA. In quiescent cells, c-myc mRNA is destabilized by the *trans*-acting complex (CPEB–Tob–Caf1), while in cells stimulated by the serum, both Tob and Caf1 are released from CPEB, and c-Myc expression is induced early after stimulation by the stabilization of its mRNA as an 'immediate-early gene'. Collectively, these results indicate that Tob is a key factor in the regulation of c-myc gene expression, which is essential for cell growth. Thus, Tob appears to function in the control of cell growth at least, in part, by regulating the expression of c-myc.

Oncogene (2014) **33,** 55–64; doi:10.1038/onc.2012.548; published online 26 November 2012

Keywords: Tob; Caf1; CPEB; mRNA decay; deadenylation

INTRODUCTION

In eukaryotes, the mRNA poly(A) tail has pivotal roles in the post-transcriptional control of gene expression. The 3′ poly(A) tail interacts with the 5′ cap to circularize mRNA, which leads to a synergistic activation of translation.[1,2] Also, shortening of the poly(A) tail, termed deadenylation, is the rate-limiting step in general mRNA decay.[3] Thus, the regulation of the poly(A) tail length contributes greatly to the control of gene expression in terms of both translation and mRNA stability.[4,5] Especially in oocyte maturation and early embryonic development, which occur in the absence of transcription, gene expression is absolutely regulated by the polyadenylation and deadenylation of maternal mRNA. In this case, CPE-containing pre-mRNA such as cyclin B1 acquires a long poly(A) tail in the nucleus that is subsequently shortened when transported to the cytoplasm. The poly(A) tail length is controlled by two cytoplasmic polyadenylation element-binding protein (CPEB)-associated proteins: a poly(A)-specific ribonuclease (PARN) deadenylase[6] and a poly(A) polymerase Gld2.[7] CPEB recruits PARN to the CPE-containing mRNA and accelerates the deadenylation reaction. Upon oocyte maturation, CPEB phosphorylation leads to the dissociation of PARN from the RNP complex and instead Gld2 associated with CPEB catalyzes default polyadenylation.[8] Thus, cytoplasmic polyadenylation activates the translation of specific mRNAs.

In somatic cells, however, poly(A) tail length is regulated mostly by deadenylation that is generally catalyzed by two major mRNA deadenylase complexes, Pan2–Pan3 and Caf1–Ccr4.[9] The former consists of the catalytic subunit Pan2 and regulatory subunit Pan3.[10] Pan3 binds to the poly(A)-binding protein PABPC1 by using the PAM2 motif and makes Pan2 accessible to the substrate poly(A), which leads to the activation of deadenylation.[10] On the other hand, both the Caf1 and Ccr4 subunits of the latter complex have the catalytic activities of the deadenylase.[11–13] The antiproliferative protein Tob forms a complex with Caf1–Ccr4[14] and mediates the binding of the deadenylases to PABPC1.[15] As in the case of Pan3, Tob binds to PABPC1 via the PAM2 motif and makes Caf1–Ccr4 accessible to the PABPC1-bound poly(A), which also leads to the activation of deadenylation.[16,17] We have previously found that the termination of translation triggers mRNA deadenylation, and proposed an initiation mechanism of mRNA decay: after translation termination, the termination complex eRF1–eRF3 is released from PABPC1, and in turn the two deadenylase complexes, Pan2–Pan3 and Caf1–Ccr4, bind to PABPC1 to degrade the poly(A) tail of the mRNA.[17] The translation termination factor eRF3 also contains PAM2 motifs, and competition between eRF3 and the two deadenylase complexes for the binding of PABPC1 is the key to this model.[17,18]

In addition to the decay of general mRNA, Tob in a complex with Caf1 also has an important role in the regulation of specific mRNA. Tob binds directly to a sequence-specific RNA-binding protein, CPEB3, and recruits Caf1 to the target of CPEB3.[19] The binding of CPEB3 to the target, AMPA receptor (GluR2) mRNA, leads to accelerated deadenylation and decay of the message and inhibition of its expression. Thus, Tob is thought to function in learning and memory by regulating the expression of the AMPA receptor.[19]

Tob is a multifunctional protein involved not only in learning and memory[20,21] but also in cell cycle progression,[22,23] spermatogenesis,[24] embryonic development,[25] osteogenesis[26]

Department of Biological Chemistry, Graduate School of Pharmaceutical Sciences, Nagoya City University, Nagoya, Japan. Correspondence: Professor S Hoshino, Department of Biological Chemistry, Graduate School of Pharmaceutical Sciences, Nagoya City University, 3-1 Tanabe-dori, Mizuho-ku, Nagoya 467-8603, Japan.
E-mail: hoshino@phar.nagoya-cu.ac.jp.
Received 1 May 2012; revised 21 September 2012; accepted 28 September 2012; published online 26 November 2012

and T-cell activation.[27] Among its known biological functions, Tob's role as a negative regulator of the cell cycle is well established. Ectopic expression of Tob or its paralog Tob2 results in the inhibition of cell proliferation.[14,22,23] Tob suppresses cyclin D1 expression upstream of Rb phosphorylation and inhibits G1-to-S phase transition.[23] However, the role of Tob in mRNA deadenylation with respect to cell growth regulation remains to be determined.

Here, we show that Tob directly regulates c-myc oncogene expression during G1-to-S phase transition. In quiescent cells, Tob forms a ternary complex CPEB–Tob–Caf1 and recruits Caf1 deadenylase to the target c-myc mRNA to degrade rapidly the message. After serum stimulation, Tob and Caf1 dissociate from CPEB, which leads to the stabilization of the mRNA and activation of its gene expression. Thus, Tob appears to function in the control of cell growth at least, in part, by regulating the expression of c-myc.

RESULTS

Tob directly binds CPEB to form a ternary complex with Caf1 deadenylase

We have previously shown that Tob directly binds to form a complex with the sequence-specific RNA-binding proteins CPEB3 and CPEB4.[19] Detailed analysis of the interaction revealed that Tob binds to the carboxyl-terminal RNA-binding domain of CPEB3/4. Since the RNA-binding domain is highly conserved among CPEB2–4 (>95% identity), and distantly related CPEB still has a homologous domain (~40–50% identity), we speculated that Tob also binds to CPEB. Thus, we first examined the interaction with a glutathione *S*-transferase (GST) pull-down assay. GST-Tob (1–285) and MBP-CPEB, which had been prepared from *Escherichia coli* with >95% purity, were mixed and pulled down by glutathione sepharose beads. Western blot analysis with anti-MBP antibody revealed the presence of MBP-CPEB, while it was not detected in the control experiment with GST (Figure 1a). The interaction was further confirmed with co-immunoprecipitation experiment. When lysate of HeLa cells expressing 5 × Flag-CPEB, 5 × Myc-Tob and 5 × Myc-Caf1 was immunoprecipitated with anti-Flag antibody, the precipitated fraction contained 5 × Myc-Tob (Figure 1b). Also, we have confirmed the presence of 5 × Myc-Caf1 in the precipitate. The precipitated amount of 5 × Myc-Caf1 was increased when 5 × Myc-Tob was expressed (Figure 1b, compare lanes 5 and 6). These interactions seemed not to be mediated by RNA since the binding experiments were performed in the presence of RNase A. These results indicate that Tob directly binds CPEB, as in the case of CPEB3 and CPEB4, to form a ternary complex with Caf1 deadenylase.

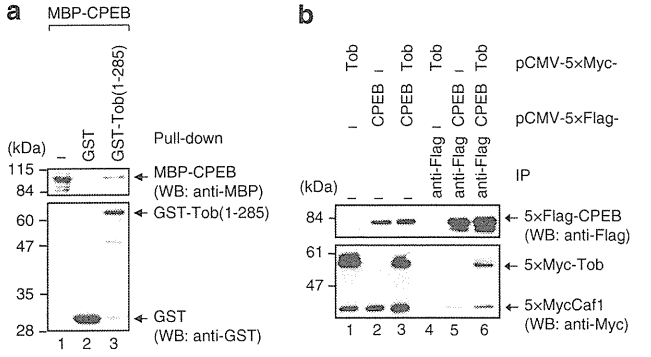

Figure 1. Tob directly binds CPEB to form a ternary complex with Caf1 deadenylase. (**a**) GST or GST-Tob was immobilized on glutathione sepharose resin and incubated with MBP-CPEB. The bound proteins (lanes 2 and 3) and the input (lane 1) were analyzed by western blotting (WB) with the indicated antibodies. (**b**) HeLa cells were transfected with pCMV-5 × Myc-Caf1, pCMV-5 × Myc-Tob, and either pCMV-5 × Flag-CPEB or pCMV-5 × Flag. The cell extracts were subjected to immunoprecipitation (IP) using anti-Flag antibody in the presence of RNase A. The immunoprecipitates (lanes 4–6) and inputs (lanes 1–3) were analyzed by western blotting with the indicated antibodies.

CPEB represses expression of c-myc 3′-UTR reporter gene by destabilizing its mRNA

The observed interaction between CPEB, Tob and Caf1 led us to speculate that CPEB's target mRNAs are regulated by deadenylation. Previous study has shown that c-myc mRNA, which contains CPEs and CPE-like sequences in its 3′-UTR (Figure 2a), is one of the targets of CPEB.[28] In an attempt to determine the significance of the interaction between CPEB, Tob and Caf1, a *β-globin* gene (BGG) reporter appended with the c-myc 3′-UTR (c-myc 3′-UTR reporter) was constructed, and the effect of CPEB on the expression of the reporter was examined by western and northern blot analyses. Exogenously expressed CPEB significantly lowered the level of BGG reporter protein in a dose-dependent manner (Figures 2b and d). This result seems not merely to be a consequence of translational repression because CPEB also reduces the level of the reporter mRNA (Figures 2c and e). The steady-state level of the reporter mRNA was reduced to ~30% by CPEB (Figure 2e), where that of the protein was reduced to ~5% (Figure 2d), suggesting that CPEB negatively regulates the reporter gene expression also at the mRNA level. The ability of CPEB to reduce the reporter mRNA and protein expression is dependent on its binding to the mRNA, as CPEB did not significantly affect the expression of the reporter gene with mutated CPEs (Figures 2b and c, lanes 4–6).

To determine whether CPEB reduces the c-myc mRNA level by promoting mRNA decay, we conducted a transcriptional pulse-chase analysis by using Tet-on system (Figure 2f). The BGG with the c-myc 3′-UTR (c-myc 3′-UTR reporter) was placed under the control of the 'Tet-on' promoter. Transcription was allowed to proceed for 2 h by adding tetracycline in T-REx HeLa cells. Cells were then washed three times to block further transcription, and total RNA was prepared from the cells sequentially after transcription was shut off. Northern blot analysis showed that the stability of c-myc 3′-UTR reporter mRNA was decreased approximately twofold by the presence of CPEB (Figures 2f and g). The signal intensity of the band was quantified along the length of the mRNA and plotted as a function of mRNA size (Figure 2h). The position of the fully deadenylated RNA (A_0) was determined by treating the steady-state mRNA with oligo (dT)/RNase H. The c-myc 3′-UTR mRNA was gradually shortened (Figure 2h, upper panel), while in cells expressing CPEB, the mRNA migrates faster to the A_0 position (Figure 2h, middle panel). The observed size difference is due to the difference in the length of the poly(A) tails, as the mRNAs were converged to the A_0 position by oligo(dT)/ RNase H treatment (Supplementary Figure S1). From these results, we conclude that CPEB accelerates deadenylation and decay of c-myc mRNA. We note that these results are not due to a secondary or nonspecific effect of CPEB, as CPEB alone did not accelerate the decay of a reporter mRNA appended with MS2-binding sites in its 3′-UTR but without CPEs (Supplementary Figure S2). On the other hand, MS2-CPEB increased the rate of deadenylation and decay for the reporter mRNA (Supplementary Figure S2). These observations further confirm that CPEB promotes deadenylation and decay of c-myc mRNA through its binding to the 3′-UTR.

Caf1 is responsible for the CPEB-accelerated decay of c-myc 3′-UTR mRNA

Next, we sought to determine whether the CPEB-accelerated decay of c-myc 3′-UTR reporter mRNA was mediated by Caf1 deadenylase. For this purpose, we applied a dominant-negative

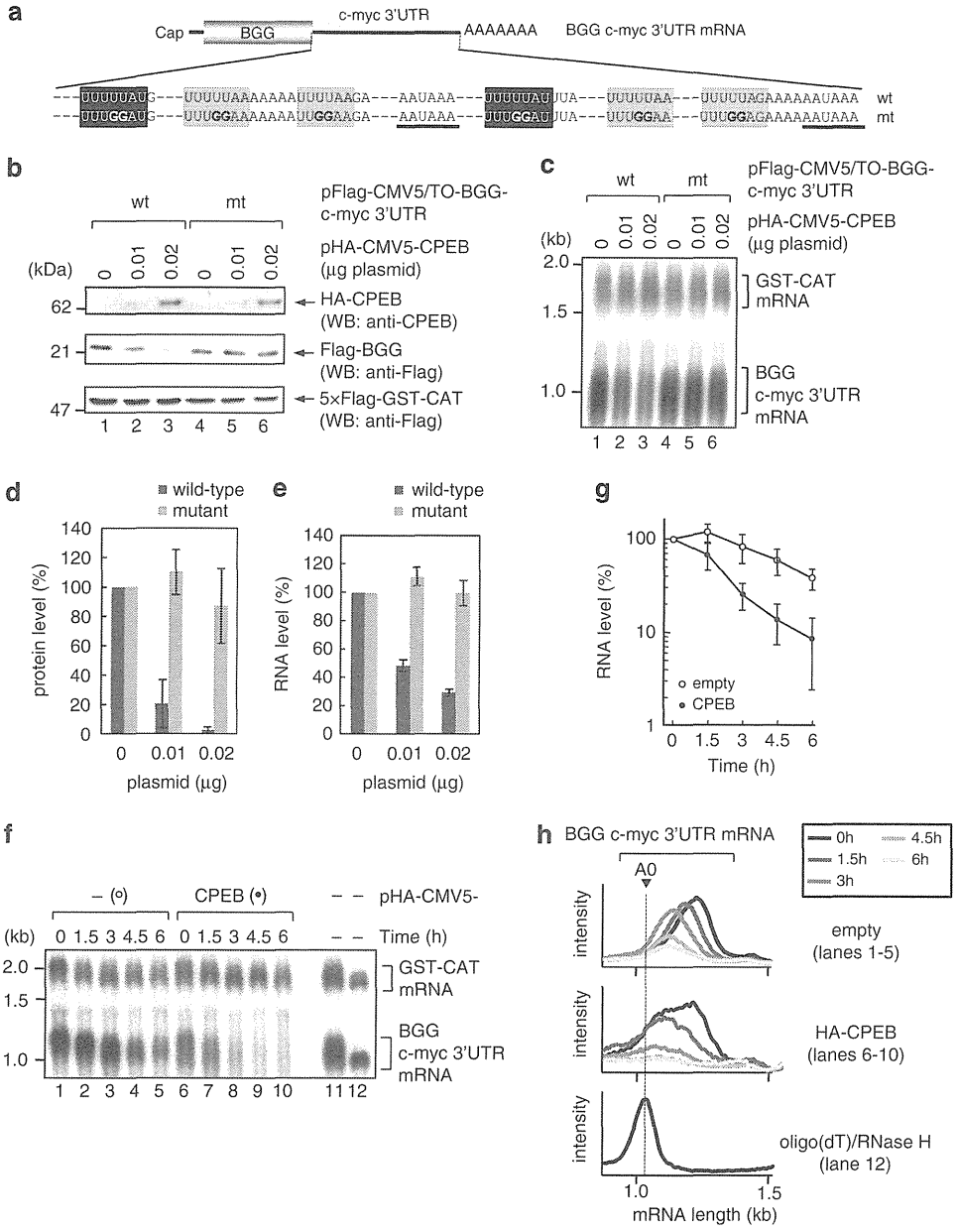

Figure 2. CPEB negatively regulates the expression of c-myc 3′-UTR reporter by promoting mRNA decay. (**a**) Schematic diagram of c-myc 3′-UTR reporter mRNA. Open reading frame of the BGG mRNA was appended with the human c-myc 3′-UTR, which contains two consensus CPEs (black box), four non-consensus CPEs (gray box) and two polyadenylation hexanucleotide sequences (black line). Bold letters designate nucleotides that were changed in the mutant reporter. (**b**) HeLa cells were transfected with increasing amounts of pHA-CMV5-CPEB, a reference plasmid pCMV-5 × Flag-GST-CAT, and either pFlag-CMV5/TO-BGG c-myc 3′-UTR (lanes 1–3) or pFlag-CMV5/TO-BGG c-myc 3′-UTR mutant (lanes 4–6). The cell extracts were subjected to western blotting (WB) with the indicated antibodies. 5 × Flag-GST-CAT served as a transfection/loading control. (**c**) HeLa cells were transfected as in (**b**). Total RNA was prepared from the cells and subjected to northern blotting. (**d**) The amount of BGG protein as in (**b**) was measured and normalized by GST-CAT protein. The score without pHA-CMV5-CPEB was defined as 100%. Data are the mean ± s.d. ($n = 3$). (**e**) The amount of BGG c-myc 3′-UTR mRNA as in (**c**) was measured and normalized by GST-CAT mRNA. The score without pHA-CMV5-CPEB was defined as 100%. Data are the mean ± s.d. ($n = 3$). (**f**) T-REx HeLa cells were co-transfected with the pFlag-CMV5/TO-BGG c-myc 3′-UTR reporter plasmid, a reference plasmid pCMV-5 × Flag-GST-CAT, and either pHA-CMV5 (lanes 1–5) or pHA-CMV5-CPEB (lanes 6–10). After 1 day, BGG mRNA was induced to express by treatment with tetracycline for 2 h, and cells were harvested at the specified time after the transcription was shut off. To analyze steady-state mRNAs, BGG mRNA was induced to express by treatment with tetracycline for 16 h (lane 11). The steady-state mRNAs were digested with *RNase*H in the presence of oligo (dT) to mark the deadenylated mRNAs (lane 12). (**g**) The level of BGG c-myc 3′-UTR mRNA as in (**f**) was quantified and normalized by the level of GST-CAT mRNA. The score from the 0 h time point was defined as 100%. Data are the mean ± s.d. ($n = 3$). (**h**) BGG c-myc 3′-UTR mRNA distribution was visualized by quantifying the signal intensity from northern blot in (**f**).

approach. T-REx HeLa cells were co-transfected with the c-myc 3′-UTR plasmid and a plasmid expressing CPEB, with or without a plasmid expressing a nuclease-deficient Caf1 mutant in which a catalytically essential aspartate residue was mutated to alanine (Caf1 D161A), and a transcriptional pulse-chase analysis was performed. The Caf1 mutant almost completely blocked CPEB-accelerated deadenylation and decay of the c-myc 3′-UTR reporter mRNA (Figures 3a and b). In contrast, a Pan2 mutant

(Pan2 D1083A) that had no deadenylase activity showed no apparent effect. The expression of comparable amounts of Caf1 D161A and Pan2 D1083A was confirmed by western blotting (Figure 3e).

In this relation, CPEB is known to bind another deadenylase PARN to regulate deadenylation of its target mRNA in the *Xenopus* oocyte.[8] The interaction was recapitulated between human-derived CPEB and PARN (Supplementary Figure S3). When lysate of HeLa cells expressing 5 × Flag-CPEB and 5 × Myc-PARN was immunoprecipitated with anti-Flag antibody, the precipitated fraction contained 5 × Myc-PARN. However, overexpression of a PARN mutant (PARN D28A) that had no deadenylase activity[29] showed no effect on CPEB-accelerated deadenylation and decay of the c-myc 3′-UTR reporter mRNA (data not shown). Collectively, these results indicate that CPEB-accelerated deadenylation and decay of the c-myc 3′-UTR reporter mRNA is dependent on the deadenylase activity of Caf1.

To confirm that Tob is involved in the CPEB-accelerated c-myc mRNA decay, small interfering RNA (siRNA)-mediated knockdown was performed. In this case, Tob and Tob2, a highly homologous paralogue of Tob, were depleted simultaneously (Figure 3f). As shown in Figures 3c and d, depletion of Tob/Tob2 significantly reduced the rate of mRNA decay of the c-myc 3′-UTR reporter.

Tob and CPEB negatively regulate endogenous c-myc expression at the mRNA level

We next examined if Tob as well as CPEB is actually involved in the regulation of endogenous c-myc mRNA. For this purpose, we used U2OS cells, as CPEB, Tob and Caf1. Proteins were all expressed in this cell line at a level sufficient for detection using our antibodies (Figure 4a). CPEB and Tob were depleted by siRNA-mediated knockdown, and the expression of c-myc was examined at both the mRNA and protein level. Depletion of Tob/Tob2 resulted in an

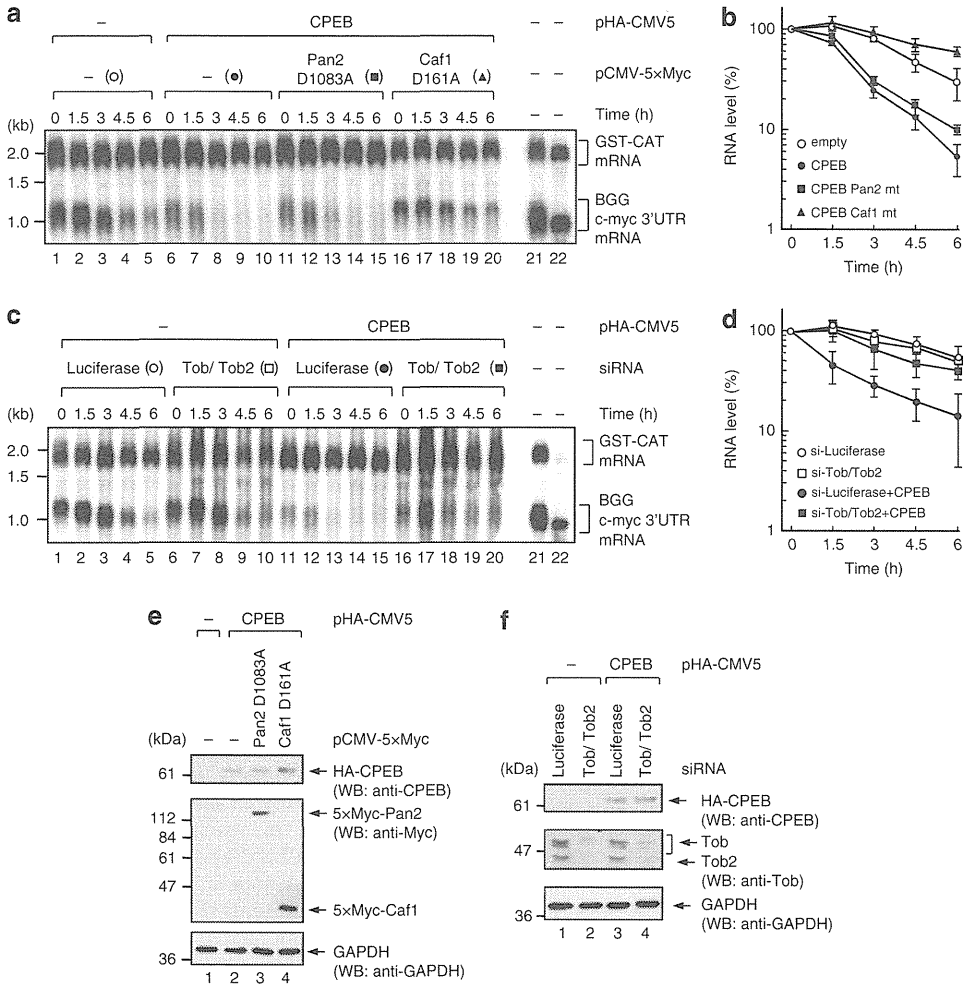

Figure 3. Tob–Caf1 complex is required for CPEB-mediated mRNA decay. (**a**) T-REx HeLa cells were transfected with the pFlag-CMV5/TO-BGG c-myc 3′-UTR reporter plasmid, pCMV-5 × Flag-GST-CAT reference plasmid, pHA-CMV5-CPEB (lanes 6–20), and either pCMV-5 × Myc-Pan2 D1083A (lanes 11–15) or pCMV-5 × Myc-Caf1 D161A (lanes 16–20). As a control, cells were transfected with pHA-CMV5 and pCMV-5 × Myc (lanes 1–5). After 1 day, BGG mRNA was induced to express by treatment with tetracycline for 2 h, and cells were harvested at the specified time after the transcription was shut off. BGG mRNA was induced to express by treatment with tetracycline for 12 h (steady state, lane 21), and digested with *RNase*H in the presence of oligo (dT) to mark the deadenylated mRNAs (lane 22). (**b**) The level of BGG c-myc 3′-UTR mRNA as in (**a**) was quantified and normalized by the level of GST-CAT mRNA. The score from the 0 h time point was defined as 100%. Data are the mean ± s.d. ($n = 3$). (**c**) HeLa cells were transfected with Tob/Tob2 or a control luciferase siRNA. At 48 h after siRNA transfection, cells were transfected with pFlag-CMV5/TO-BGG c-myc 3′-UTR reporter plasmid, pCMV-5 × Flag-GST-CAT reference plasmid, pcDNA-T7-TetR, and either pHA-CMV5-CPEB (lanes 11–20) or pHA-CMV5 (lanes 1–10). The transcriptional pulse-chase analysis was performed as described above. (**d**) The level of BGG c-myc 3′-UTR mRNA as in (**c**) was quantified and normalized by the level of GST-CAT mRNA. The score from the 0 h time point was defined as 100%. Data are the mean ± s.d. ($n = 3$). (**e**, **f**) Total cell lysate was analyzed by western blotting (WB) using indicated antibodies.

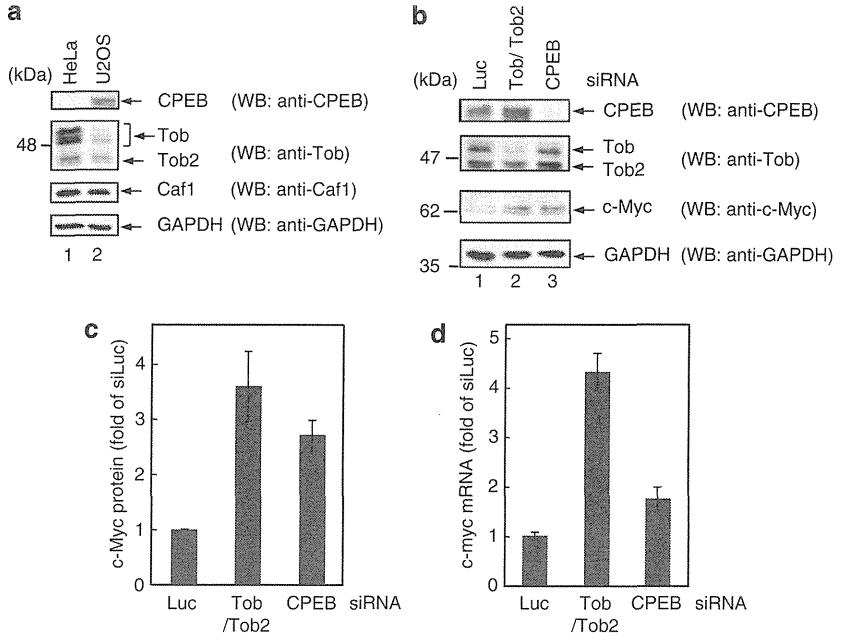

Figure 4. Downregulation of CPEB or Tob/Tob2 increases the levels of endogenous c-myc mRNA and protein in U2OS cells. (**a**) Whole cell lysate from U2OS or HeLa cells was analyzed by western blotting (WB) using the indicated antibodies. (**b**) U2OS cells were transfected with Tob/Tob2 siRNA, CPEB siRNA or a control luciferase siRNA. At 72 h after transfection, cells were harvested and total cell lysate was analyzed by WB using indicated antibodies. (**c**) The amount of c-Myc protein as in (**b**) was measured and normalized by GAPDH. The c-Myc protein level in luciferase siRNA-treated cells was set to 1 and fold-increases are indicated. Data are the mean ± s.d. ($n = 3$). (**d**) U2OS cells were transfected with Tob/Tob2 siRNA, CPEB siRNA or a control luciferase siRNA. At 72 h after transfection, total RNA was isolated and reverse-transcribed using random primer, and endogenous c-myc and GAPDH mRNA levels were analyzed by real-time PCR. The c-myc mRNA levels were normalized by GAPDH mRNA, and fold-increases are indicated with the c-myc mRNA level in luciferase siRNA-treated cells set to 1. Data are the mean ± s.d. ($n = 3$).

approximately three- to fourfold increase in c-myc expression at both levels (Figures 4b–d). Similar results were obtained for CPEB. c-myc expression at both the protein and mRNA level was increased by the depletion of CPEB, although relatively modestly (two- to threefold) (Figures 4b–d). These results indicate that CPEB and Tob form a ternary complex (CPEB–Tob–Caf1) and negatively regulate c-myc mRNA in cells.

Tob/Tob2 and CPEB negatively regulate the stability of endogenous c-myc mRNA in starved cells and the effects are abrogated by serum stimulation

It is well established that the level of c-myc mRNA depends upon the cellular growth state. In serum-starved cells, c-myc mRNA is expressed at a very low level. When cells are stimulated by serum, the abundance of c-myc mRNA starts to rise, and peaked within 1 and 2 h, followed by a decline and a plateau at several fold the levels in starved cells.[30] The transcription level reaches a peak before that of the c-myc mRNA level. As both Tob and CPEB regulate cell cycle progression, we examined whether these factors are involved in the serum-induced immediate-early response of c-myc gene expression (Figures 5b and c). To measure changes in the level of c-myc transcription and mRNA abundance at the same time, we performed a real-time polymerase chain reaction (PCR) analysis using two pairs of PCR primers (Figure 5a) and reverse transcription (RT) products of total RNA prepared from U2OS cells as a template. The primer pair a–c amplifies c-myc mature mRNA (cytoplasmic mRNA), whereas primer pair b and c amplifies c-myc pre-mRNA (nuclear mRNA). The pre-mRNA level generally reflects transcription. It is important to note that even after 35 thermal cycles, no amplification was observed when mock RT products prepared without reverse transcriptase were used as a template, and that these primer pairs amplify only a single band (Supplementary Figure S4A and data not shown). As shown in SupplementaryFigure S4B, the c-myc transcription and mRNA abundance measured in this assay system faithfully recapitulated the fluctuations previously reported upon serum stimulation, further validating the specificity of the primer pairs. Similar to the results from the steady-state analysis in Figure 4, knockdown of either Tob/Tob2 or CPEB resulted in a marked increase in c-myc mature mRNA in starved cells (Figure 5b, mature mRNA, starved, $P < 0.05$). However, the effect was attenuated at 1 h after serum stimulation (Figure 5b; mature mRNA, stimulated), suggesting that Tob/Tob2 and CPEB negatively regulate the level of c-myc mRNA under starved conditions and the effects are abrogated by serum stimulation. Analysis of pre-mRNA revealed that knockdown of Tob/Tob2 but not CPEB increased c-myc transcription slightly but significantly in starved condition (Figure 5b; pre-mRNA, $P < 0.05$). This result explains why c-myc mRNA was more abundant in Tob/Tob2 knockdown cells than in CPEB knockdown cells (Figure 4d). Figure 5c shows the same result as in Figure 5b, but the *y* axis represents the fold-increase of c-myc mature or pre-mRNA in serum-stimulated cells relative to starved cells. In control siRNA-treated cells, c-myc mature mRNA was increased by ~7-fold (Figure 5c, Luc, 2nd column). Knockdown of either Tob/Tob2 or CPEB reduced c-myc mRNA induction by ~3-fold after serum stimulation (Figure 5c; Tob/Tob2, CPEB, 2nd column, $P < 0.005$). In contrast, there were no significant differences in the induction of c-myc pre-mRNA among these cells (Figure 5c; Tob/Tob2, CPEB, 4th column). Consistent with fluctuations of c-myc mRNA, c-Myc protein was increased by knockdown of either Tob or CPEB in starved cells (Figures 5d and e). Also, serum-stimulated induction of c-Myc protein was inhibited by their knockdowns (Figures 5d and f). These results strengthen our conclusion that CPEB and Tob regulate the expression of c-Myc at the level of mRNA.

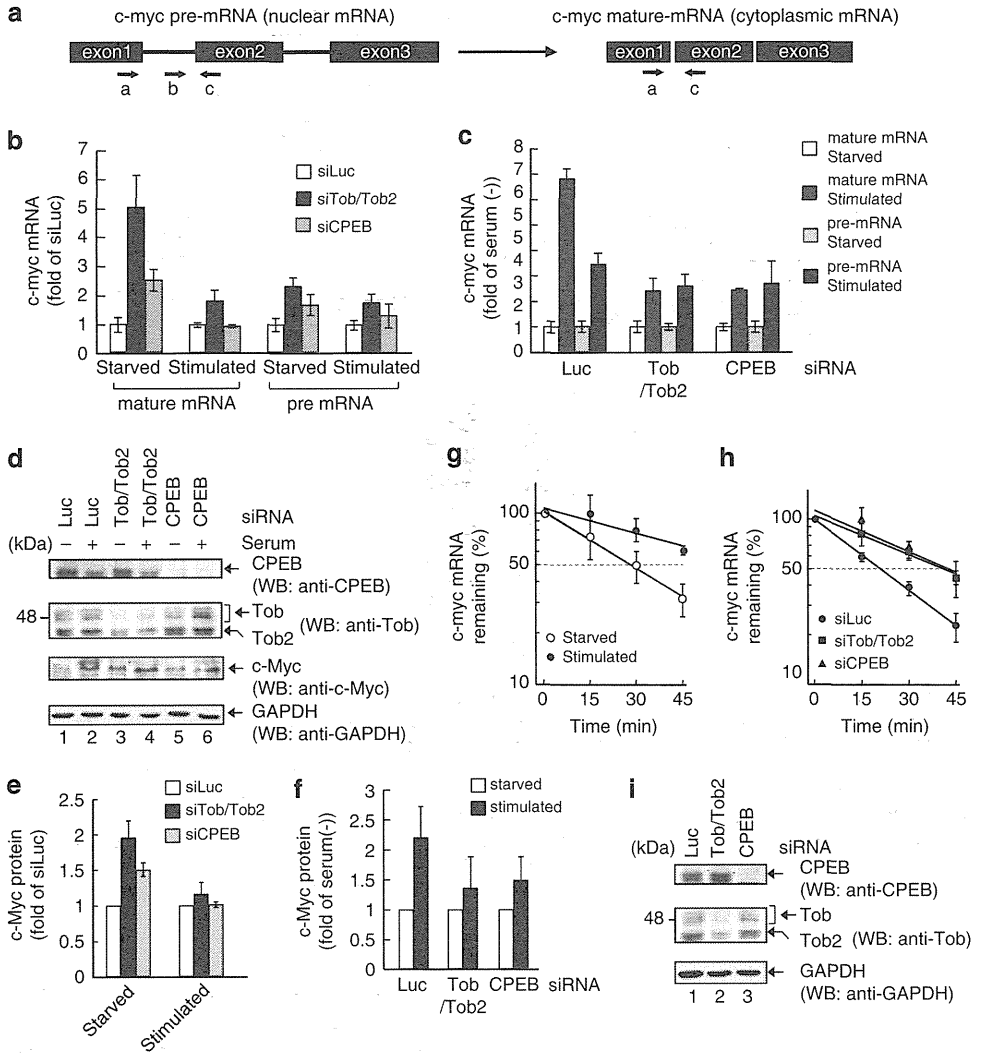

Figure 5. Tob/Tob2 and CPEB negatively regulate the stability of endogenous c-myc mRNA under starved conditions and the effects are abrogated by serum stimulation. (**a**) Diagram of c-myc mRNA and primers used for real-time PCR. Sense primers a and b correspond to sites within exon 1 and intron 1, respectively. Antisense primer c corresponds to exon 2. In this study, c-myc pre- and mature mRNA were amplified with primer pairs b–c and a–c, respectively. (**b**) U2OS cells were transfected with Tob/Tob2 siRNA, CPEB siRNA or a control luciferase siRNA. At 48 h after transfection, cells were washed and serum-starved for 24 h. Quiescent cells were stimulated with 10% fetal bovine serum (FBS) for 1 h, and total RNA was isolated and reverse-transcribed using random primer. Endogenous c-myc pre- and mature mRNA levels were analyzed by real-time PCR. The c-myc mRNA levels were normalized by GAPDH mRNA, and fold-increases are indicated with the c-myc mRNA level in luciferase siRNA-treated cells set to 1. Data are the mean ± s.d. ($n = 3$). (**c**) Data in (**b**) were analyzed and expressed with serum-starved samples set to 1. (**d**) U2OS cells were transfected with Tob/Tob2 siRNA, CPEB siRNA or a control luciferase siRNA. Total cell lysates were analyzed by western blotting (WB) using indicated antibodies. (**e**) The amount of c-Myc protein as in (**d**) was measured and normalized by GAPDH. The score in luciferase siRNA-treated cells was set to 1 and fold-increases are indicated. Data are the mean ± s.d. ($n = 3$). (**f**) Data in (**d**) were analyzed and expressed with serum-starved samples set to 1. (**g**) U2OS cells were washed and serum-starved for 24 h. Quiescent cells were pre-treated with 10 μg/ml actinomycin D for 15 min, and stimulated with 10% FBS or left untreated. Total RNA was isolated at the indicated times and reverse-transcribed using random primer. Endogenous c-myc mRNA levels (normalized by GAPDH mRNA) were analyzed by real-time PCR. The c-myc mRNA half-lives were 27.6 and 62.2 min in starved and stimulated cells, respectively. Data are the mean ± s.d. ($n = 3$). (**h**) U2OS cells were transfected with Tob/Tob2 siRNA, CPEB siRNA or a control luciferase siRNA. At 48 h after transfection, cells were washed and serum-starved for 24 h. Quiescent U2OS cells were treated with 10 μg/ml actinomycin D and 10% FBS. Total RNA was isolated and c-myc mRNA levels (normalized by GAPDH mRNA) were analyzed. The c-myc mRNA half-lives were 21.2, 38.8 and 37.0 min in control, Tob/Tob2 and CPEB knockdown cells, respectively. Data are the mean ± s.d. ($n = 3$). (**i**) Total cell lysate was analyzed by WB using indicated antibodies.

The above results led us to speculate that both Tob/Tob2 and CPEB are involved in the induction of c-myc mRNA expression after serum stimulation in a process of controlling mRNA stability. To investigate this possibility, we first examined if there are changes in c-myc mRNA stability after serum stimulation. Serum-starved U2OS cells were pre-treated with actinomycin D for 15 min, and then stimulated with serum or left untreated (starved). Actinomycin D was maintained in the medium throughout the time course. Total RNA was isolated every 15 min after serum was added and analyzed by real-time PCR. As shown in Figure 5g, the half-life of c-myc mRNA was about 2.3-fold longer in stimulated cells than starved cells. Thus, we next estimated the half-life of c-myc mRNA in serum-starved quiescent cells that were treated with siRNA against either Tob/Tob2 or CPEB (Figures 5h and i).

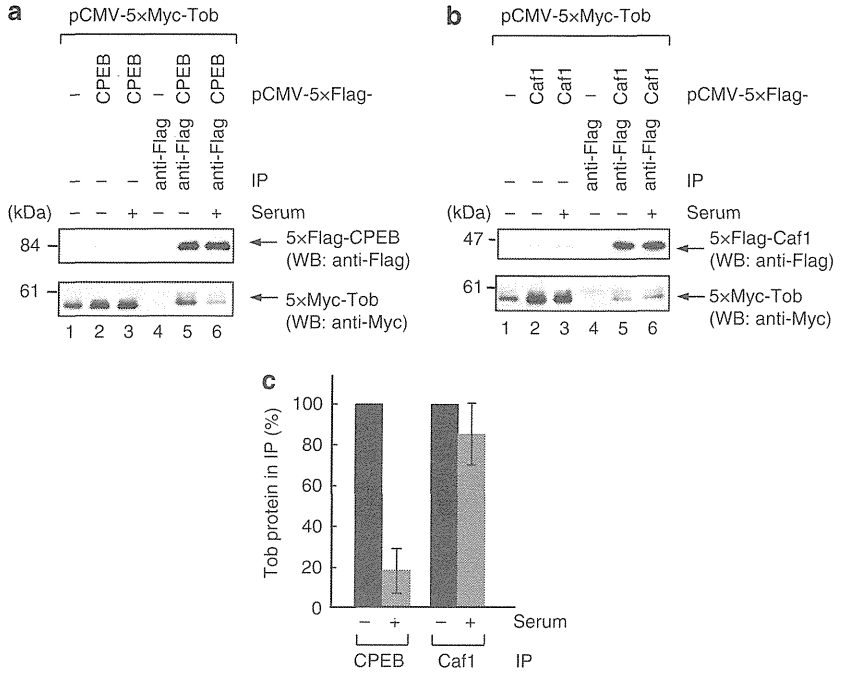

Figure 6. Serum stimulation induces dissociation of Tob and Caf1 from CPEB. (**a**) U2OS cells were transfected with pCMV-5 × Myc-Tob, and either pCMV-5 × Flag-CPEB or pCMV-5 × Flag. After 1 day, cells were washed and serum-starved for 24 h. The quiescent cells were stimulated with 10% fetal bovine serum (FBS) for 20 min and cell extracts were subjected to immunoprecipitation (IP) in the presence of *RNase*I using anti-Flag antibody. The immunoprecipitates (lanes 4–6) and inputs (lanes 1–3) were analyzed by western blotting with the indicated antibodies. (**b**) U2OS cells were transfected with pCMV-5 × Myc-Tob, and either pCMV-5 × Flag-Caf1 or pCMV-5 × Flag. After 1 day, cells were washed and serum-starved for 24 h. The quiescent cells were stimulated with 10% serum for 20 min and cell extracts were subjected to IP in the presence of *RNase*I using anti-Myc antibody. The immunoprecipitates (lanes 4–6) and inputs (lanes 1–3) were analyzed by western blotting with the indicated antibodies. (**c**) The amounts of the co-purified Tob proteins in the immunoprecipitates as in (**a**) and (**b**) were quantified and normalized by the amount of CPEB or Caf1 proteins immunoprecipitated. The score from serum-starved cells was defined as 100%. Data are the mean ± s.d ($n = 3$).

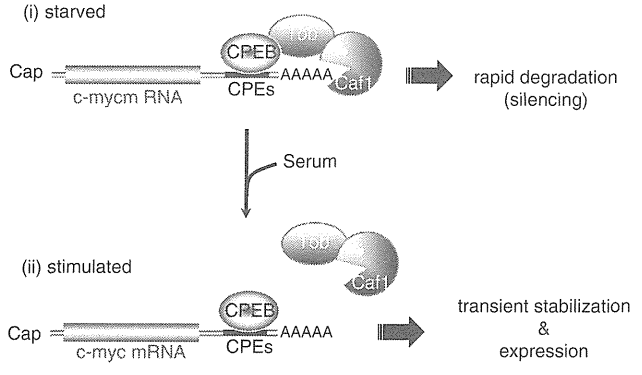

Figure 7. Proposed model for the serum-induced stabilization of c-myc mRNA. In serum-starved quiescent cells, CPEB bound to the *cis* elements (CPEs) in the c-myc mRNA 3′-UTR recruits the Tob–Caf1 complex to the mRNA to form a ternary complex, which leads to accelerated deadenylation and decay of the message. Upon serum stimulation, Tob and Caf1 transiently dissociate from CPEB and c-myc mRNA is stabilized and expressed as an 'immediate-early response gene'.

The half-life was extended in both Tob/Tob2 and CPEB knockdown cells by about twofold, near comparable to that in stimulated cells (2.3-fold as described above).

Tob and Caf1 dissociate from CPEB in response to serum stimulation

Finally, we performed co-immunoprecipitation experiments in serum-starved and -stimulated cells. When lysate of serum-starved U2OS cells expressing 5 × Flag-CPEB and 5 × Myc-Tob was immunoprecipitated with anti-Flag antibody, the precipitated fraction contained 5 × Myc-Tob as well as 5 × Flag-CPEB, whereas association of 5 × Myc-Tob with 5 × Flag-CPEB was drastically decreased after serum stimulation (Figures 6a and c, lanes 4–6, $P < 0.005$). In contrast, when lysate of serum-starved U2OS cells expressing 5 × Flag-Caf1 and 5 × Myc-Tob was immunoprecipitated with anti-Flag antibody, 5 × Myc-Tob was co-precipitated with 5 × Flag-Caf1 irrespective of the presence or absence of the serum, indicating that the binding of Tob with Caf1 was not affected by the serum condition (Figures 6b and c, lanes 4–6).

Taken together, our observations demonstrate that CPEB accelerates deadenylation and decay of the c-myc mRNA by recruiting the Tob–Caf1 complex to c-myc mRNA in starved quiescent cells, and serum stimulation induces dissociation of the Tob–Caf1 complex from CPEB to stabilize c-myc mRNA.

DISCUSSION

Tob is a member of the BTG/Tob family of antiproliferative proteins, which regulates cell cycle progression in a variety of cell types. Previous study demonstrated that Tob is involved in the control of G1- to S-phase transition of the cell cycle.[22,23] On the other hand, we and others have demonstrated that Tob functions in deadenylation of both general[16,17] and specific[19] mRNAs. However, the role of Tob in mRNA deadenylation with respect to cell growth regulation has remained to be determined.

This study provides evidence that Tob mediates deadenylation of c-myc mRNA and negatively regulates its expression. In serum-starved quiescent state, Tob mediates recruitment of Caf1 deadenylase to the CPEB-bound c-myc mRNA and accelerates deadenylation and decay of the mRNA. While in cells stimulated

by serum, Tob in a complex with Caf1 dissociates from CPEB-bound c-myc mRNA, which leads to a transient stabilization of the message and immediate-early expression of c-Myc (Figure 7). Thus, Tob appears to function in the control of cell growth at least, in part, by regulating the expression of c-myc.

It has been reported that CPEB activates translation of CPE-containing mRNAs (for example, αCAMKII and p53) by promoting cytoplasmic polyadenylation of the messages.[31,32] In contrast, no CPE-containing mRNA that is subject to accelerated deadenylation by CPEB has been reported in mammalian somatic cells. To our knowledge, c-myc is the first example of such an mRNA. Therefore, it was surprising that tethering CPEB to mRNA 3′-UTR led to accelerated deadenylation and decay of the mRNA (Supplementary Figure S2), which is reminiscent of c-myc, but neither αCAMK2 nor p53. Moreover, reporter mRNAs appended with other CPEB-target 3′-UTR, such as c-jun 3′-UTR,[33] were not affected by overexpression of CPEB (data not shown). Thus, CPEB does not necessarily induce polyadenylation (or deadenylation) of CPE-containing mRNAs by default. It remains unknown what determines whether CPEB-bound mRNAs will be degraded by accelerated deadenylation or translationally activated by cytoplasmic polyadenylation. In *Xenopus* oocytes, not every CPE-containing mRNA is translationally activated at the same time during meiosis after progesterone treatment. The positional distribution and the number of CPE sequences, as well as the arrangement of other *cis*-acting elements, such as AU-rich element,[34] Musashi-binding element,[35] Pumilio-binding element[36] and translational control sequence,[37] around CPEs define the extent and timing of translational activation.[38] Moreover, translational repression by CPEB requires a cluster of at least two CPEs with an optimal distance of 10–12 nucleotides.[36] This finding implies that the recruitment of the translational repressor maskin is mediated by a CPEB dimer formed on two adjacent CPEs. It is possible that such factors are involved in the determination of the fate of CPE-containing mRNAs in mammalian somatic cells. We are currently investigating this possibility.

c-Myc is a basic helix–loop–helix leucine zipper transcription factor and is required for the activation of cyclin D-dependent kinases and G0/G1- to S-phase transition.[39] Numerous studies have documented that the c-myc oncogene is expressed immediately after growth stimulation of quiescent cells and is essential for the regulation of cell growth. In most cases, changes measured in the rate of c-myc gene transcription are insufficient to account for the fluctuations and even no significant change in the rate of transcription was detectable in some cells.[30,40,41] These results suggest that the changes in c-myc expression during G0/G1- to S-phase transition are controlled by a post-transcriptional mechanism. However, this mechanism has remained to be determined for over 20 years. The results presented here provide one answer to this long-standing question.

Activation of c-myc gene expression after mitogenic stimulation is mediated by the Ras/Raf/mitogen-activated protein kinase pathway.[42] In this relation, previous study demonstrated that Tob is phosphorylated at serine residues by mitogen-activated protein kinase (Erk1/Erk2) downstream of the Ras signaling pathway.[22,23] These results led us to speculate that serum activates Ras-mitogen-activated protein kinase signaling pathways and the Erk-mediated phosphorylation of the serine residues of Tob is responsible for the dissociation of Tob from CPEB and stabilization of c-myc mRNA. However, mutant Tob with either serine-to-alanine or serine-to-glutamate mutations at the Erk phosphorylation sites (Ser 152, 154 and 164) bound CPEB with similar affinity to wild-type Tob and still showed dissociation from CPEB upon serum stimulation (data not shown). Previous study demonstrated that Tob is phosphorylated at at least three serine/threonine residues other than Ser 152, 154 and 164 upon mitogenic stimulation.[23] Thus, phosphorylation of residues other than the three serine residues or other modifications of Tob and/or CPEB seem to be responsible for the dissociation of the complex.

In addition to Tob and c-Myc, CPEB and Caf1 are also known to be involved in cell cycle regulation. (i) siRNA-mediated knockdown of CPEB results in an increase in astrocytic cell proliferation, whereas overexpression of CPEB inhibits it.[43] On the other hand, similar CPEB knockdown shows proliferation defects in HeLa cells.[44] (ii) siRNA-mediated knockdown of Caf1 leads to a defect in both G1- to S-phase transition and cell proliferation,[45] while overexpression of Caf1 also inhibits cell proliferation.[46] Thus, as in the case for Tob, Caf1 and CPEB also inhibit cell proliferation when overexpressed in cells, but the phenotypes resulting from siRNA-mediated knockdowns are divergent depending on cell types and on each component. Since CPEB also regulates cytoplasmic polyadenylation of cell cycle regulators (for example, CDKN3, Mnt, STXBP2, and so on) and Caf1 regulates transcription and deadenylation of general mRNAs, the effect on proliferation resulting from the modulation of these components might not be unidirectional.

Previous studies have shown that CPEB promotes polyadenylation-induced translational activation of cyclin B1 mRNA in the M phase and maskin-mediated translational repression in the S phase of early mitotic cell divisions in *Xenopus* embryos.[47] In contrast to the early embryonic divisions without intervening G1 and G2 phases, CPEB also regulates G2- to M-phase transition of mitotically dividing cells by mediating cytoplasmic polyadenylation of specific mRNAs, including CDKN3 and Cdc20.[44] In this study, we have shown that CPEB-mediated deadenylation and decay of c-myc mRNA might also be important for the regulation of G0/G1- to S-phase transition of the cell cycle. Remaining questions that we are currently pursuing are whether CPEB promotes cytoplasmic polyadenylation not only in the M phase but also during G0/G1- to S-phase transition and whether c-myc mRNA is polyadenylated in response to serum stimulation in a CPEB-dependent manner. These will be the subjects of forthcoming papers.

MATERIALS AND METHODS

Plasmids

To construct pHA-CMV5-CPEB, pCMV-5 × Myc-CPEB, pCMV-5 × Flag-CPEB, pMAL-cRI-CPEB and pGEX6P1-CPEB, the full-length open reading frame was PCR-amplified using the primers: sense, 5′-TTTCAATTGATG GCGTTCCCGCTGGAA-3′ and antisense, 5′-TTTGTCGACCTAGCTGGAA TCTCGGTTC-3′, and CPEB1 cDNA (IMAGE i.d. no. 6047179; Thermo Fischer Scientific, Waltham, MA, USA) as a template. The resulting DNA was digested with *Mun*I and *Sal*I and inserted into *Eco*RI and *Sal*I sites of pHA-CMV5, pCMV-5 × Myc, pCMV-5 × Flag, pMAL-cRI (New England Biolaboratories, Ipswich, MA, USA) and pGEX6P1 (GE Healthcare, Waukesha, WI, USA), respectively. To generate pCMV-5 × Myc-Tob, pME-Myc-Tob[19] was digested with *Eco*RI, and Tob cDNA fragment was inserted into the *Eco*RI site of pCMV-5 × Myc. To construct pCMV-5 × Myc-PARN, full-length PARN open reading frame was PCR-amplified using the primers: sense, 5′-A AGGTCGACATGGAGATAATCAGGAGC-3′ and antisense, 5′-AGAGTCGA CTTACCATGTGTCAGGAAC3′, and HeLa oligo(dT)-primed RT products. The resulting fragments were digested with *Sal*I and inserted into pCMV-5 × Myc. To construct pFlag-CMV5/TO-BGG c-myc 3′-UTR, pFlag-CMV5/TO-BGG(*Hind*III) was generated by introducing a *Hind*III site into the stop codon of pFlag-CMV5/TO-BGG using the primers: 5′-CTTGCTTTCTTG CTGTCCAATTTC-3′ and 5′-CTTAGTGATACTTGTGGGCCAGGG-3′. c-myc 3′-UTR was PCR-amplified using: sense, 5′-GAAAGCTTGTTCTAGAGG AAAAGTAAGGAA-3′ and antisense, 5′-GACGGTAGGATCCAGCTGGCTGCA GGTGAG-3′, and HeLa genomic DNA as a template. The resulting DNA was digested with *Hind*III and *Pst*I and inserted into pFlag-CMV5/TO-BGG(*Hind*III). To generate pFlag-CMV5/TO-BGG c-myc 3′-UTR CPE mt, the 3′, middle and 5′ segments of c-myc 3′-UTR were PCR-amplified using the following primer pairs: sense, 5′-GAAAGCTTGTTCTAGAGGAAAAGTAA GGAA-3′ and antisense, 5′-GTAAGCATCCAAAAGTTCTTTTATGCCCAA-3′; sense, 5′-AAGAACTTTTGGATGCTTACCATCTTTTTT-3′ and antisense, 5′-ACTT AAATCCAAAAAATTAGGGTTTATAGT-3′; and sense, 5′-CTAATTTTTTGGATT TAAGTACATTTTGCT-3′ and antisense, 5′-GACGGTAGGATCCAGCTGGC

TGCAGGTGAG-3′, respectively, and pFlag-CMV5/TO-BGG c-myc 3′-UTR as a template. The amplified fragments were mixed and used as a template for the second PCR conducted to generate full-length c-myc 3′-UTR fragment. The resulting fragment was digested with *Hind*III and *Pst*I and inserted into pFlag-CMV5/TO-BGG 3′-UTR(*Hind*III). The construction of pGEX6P1-Tob (1–285), pCMV-5 × Myc-Pan2 D1083A and pCMV-5 × Myc Caf1 D161A was described previously.[19]

siRNA

The sequences of siRNAs for luciferase, Tob and Tob2 were described previously.[19] CPEB siRNA consists of 5′-r (GACUCUGAAGAAACAGUUA) d(TT)-3′.

Antibodies

Antibodies used in this study were the following: anti-Flag (M2; Sigma, St Louis, MO, USA), anti-c-Myc (9E10 (Roche, Indianapolis, IN, USA); A-14, C-33 (Santa Cruz Technology, Santa Cruz, CA, USA)), anti-glyceraldehyde 3-phosphate dehydrogenase (GAPDH) (6C5; Millipore, Bedford, MA, USA), anti-GST (Z-5, Santa Cruz Technology), anti-MBP (New England Biolaboratories). Anti-Tob was raised against His-tagged Tob (1–110 amino acids). Anti-Caf1 (for immunoprecipitation), anti-CPEB and anti-PABPC1 were raised against His-tagged full-length proteins. Anti-Caf1 was a gift from Ann-Bin Shyu.[16]

Cell culture and transfection

HeLa, T-REx HeLa and U2OS cells were cultured in Dulbecco's modified Eagle's medium (Nissui, Tokyo, Japan) supplemented with 5% fetal bovine serum. U2OS cells were purchased from ATCC. DNA transfection was performed using Lipofectamine 2000 (Invitrogen, Carlsbad, CA, USA) as described previously.[17] For siRNA transfection, Lipofectamine RNAi MAX (Invitrogen) was used. For transfection with both siRNA and plasmid DNA, cells were first transfected with siRNA using RNAi MAX. After 24 h, cells were trypsinized, and re-cultured for another 24 h before DNA transfection using Lipofectamine 2000. Following further incubation for 24 h, pulse-chase experiments were conducted.

Immunoprecipitation

For immunoprecipitations, cells were lysed with 10 μg/ml RNaseA (Sigma) or 50 U/ml RNase I (New England Biolaboratories) in lysis buffer consisting of 50 mM Tris-HCl (pH 7.5), 50 mM NaCl, 0.25% Nonident P-40, 1 mM dithiothreitol, 2.5 mM ethylenediaminetetraacetic acid, 20 mM NaF, 10 mM $Na_4P_2O_7$, 0.1 mM phenylmethanesulfonylfluoride, 2 μg/ml aprotinin, and 2 μg/ml leupeptin. After centrifugation at 15 000 *g* for 20 min, the supernatant was incubated for 2 h at 4 °C with anti-Flag IgG agarose (Sigma), or anti-Myc agarose (Sigma). The resin was then washed three times with lysis buffer, and proteins retained on the resin were subjected to sodium dodecyl sulfate-polyacrylamide gel electrophoresis and western blot analysis.

GST-pull-down assay

GST-fused Tob and MBP-CPEB were produced in *E. coli* BL21 by adding 0.4 mM isopropylthio-β-galactoside and purified as described previously.[19] GST-fused Tob and MBP-CPEB were incubated with glutathione sepharose 4B (GE Healthcare) for 2 h at 4 °C in binding buffer (20 mM Tris-HCl (pH 7.5), 50 mM NaCl, 0.5% Nonident P-40, 1 mM dithiothreitol, 2.5 mM ethylenediaminetetraacetic acid). The resin was then washed three times with binding buffer. Bound proteins were eluted with sodium dodecyl sulfate-polyacrylamide gel electrophoresis sample buffer and analyzed by western blotting.

Northern blot analysis

The northern blot analysis, transcriptional pulse-chase analysis and oligo (dT)-RNase H treatment of mRNA to generate poly(A)$^-$ mRNA were performed as described previously,[19] except that the pulse transcription was induced by 10 ng/ml tetracycline for 2 h.

Real-time PCR analysis

Cells were directly harvested (steady-state level) or treated with 10 μg/ml actinomycin D (mRNA decay) and harvested at indicated times. Total RNA was isolated by the acid guanidinium–phenol–chloroform method with minor modifications and genomic DNA was removed by digestion with DNase I for 30 min. Random-primed RT of RNA (1.5 μg) was performed using SuperScript III Reverse Transcriptase (Invitrogen). Real-time PCR analysis was performed using StepOne Real-Time PCR system with PowerSYBR Green PCR Master Mix (Applied Biosystems, Foster City, CA, USA). Changes in c-myc mRNA levels were determined by the relative standard curve method using GAPDH mRNA for internal normalization. The primers for GAPDH were described previously.[19] c-myc mRNA was amplified using primers: sense, 5′-TTCGGGTAGTGGAAAACCAG-3′ and antisense, 5′-GGAACTATGACCTCGACTACGACT-3′. C-myc pre-mRNA was amplified using: sense, 5′-GCACCAAGACCCCTTTAACT-3′ and antisense, 5′-GGAAC;TATGACCTCGACTACGACT-3′. The specificity of the primer pairs and genomic DNA digestion were checked by PCR analysis using KOD FX (TOYOBO, Osaka, Japan) or PowerSYBR Green (Applied Biosystems).

CONFLICT OF INTEREST

The authors declare no conflict of interest.

ACKNOWLEDGEMENTS

We thank A-B Shyu for anti-Caf1 antibody. This work was supported by a Grant-in-Aid for Scientific Research on Innovative Areas 'RNA regulation' (No. 20112006) from the Ministry of Education, Culture, Sports, Science and Technology of Japan.

REFERENCES

1 Gallie DR. The cap and poly(A) tail function synergistically to regulate mRNA translational efficiency. *Genes Dev* 1991; **5**: 2108–2116.
2 Iizuka N, Najita L, Franzusoff A, Sarnow P. Cap-dependent and cap-independent translation by internal initiation of mRNAs in cell extracts prepared from *Saccharomyces cerevisiae*. *Mol Cell Biol* 1994; **14**: 7322–7330.
3 Decker CJ, Parker R. A turnover pathway for both stable and unstable mRNAs in yeast: evidence for a requirement for deadenylation. *Genes Dev* 1993; **7**: 1632–1643.
4 Wu X, Brewer G. The regulation of mRNA stability in mammalian cells: 2.0. *Gene* 2012; **500**: 10–21.
5 Eckmann CR, Rammelt C, Wahle E. Control of poly(A) tail length. *Wiley Interdiscip Rev RNA* 2011; **2**: 348–361.
6 Korner CG, Wormington M, Muckenthaler M, Schneider S, Dehlin E, Wahle E. The deadenylating nuclease (DAN) is involved in poly(A) tail removal during the meiotic maturation of *Xenopus* oocytes. *EMBO J* 1998; **17**: 5427–5437.
7 Barnard DC, Ryan K, Manley JL, Richter JD. Symplekin and xGLD-2 are required for CPEB-mediated cytoplasmic polyadenylation. *Cell* 2004; **119**: 641–651.
8 Kim JH, Richter JD. Opposing polymerase-deadenylase activities regulate cytoplasmic polyadenylation. *Mol Cell* 2006; **24**: 173–183.
9 Yamashita A, Chang TC, Yamashita Y, Zhu W, Zhong Z, Chen CY *et al.* Concerted action of poly(A) nucleases and decapping enzyme in mammalian mRNA turnover. *Nat Struct Mol Biol* 2005; **12**: 1054–1063.
10 Uchida N, Hoshino S, Katada T. Identification of a human cytoplasmic poly(A) nuclease complex stimulated by poly(A)-binding protein. *J Biol Chem* 2004; **279**: 1383–1391.
11 Bianchin C, Mauxion F, Sentis S, Seraphin B, Corbo L. Conservation of the deadenylase activity of proteins of the Caf1 family in human. *RNA* 2005; **11**: 487–494.
12 Chen J, Chiang YC, Denis CL. CCR4 a 3′–5′ poly(A) RNA and ssDNA exonuclease, is the catalytic component of the cytoplasmic deadenylase. *EMBO J* 2002; **21**: 1414–1426.
13 Viswanathan P, Ohn T, Chiang YC, Chen J, Denis CL. Mouse CAF1 can function as a processive deadenylase/3′–5′-exonuclease in vitro but in yeast the deadenylase function of CAF1 is not required for mRNA poly(A) removal. *J Biol Chem* 2004; **279**: 23988–23995.
14 Ikematsu N, Yoshida Y, Kawamura-Tsuzuku J, Ohsugi M, Onda M, Hirai M *et al.* Tob2, a novel anti-proliferative Tob/BTG1 family member, associates with a component of the CCR4 transcriptional regulatory complex capable of binding cyclin-dependent kinases. *Oncogene* 1999; **18**: 7432–7441.
15 Okochi K, Suzuki T, Inoue J, Matsuda S, Yamamoto T. Interaction of anti-proliferative protein Tob with poly(A)-binding protein and inducible poly(A)-binding protein: implication of Tob in translational control. *Genes Cells* 2005; **10**: 151–163.
16 Ezzeddine N, Chang TC, Zhu W, Yamashita A, Chen CY, Zhong Z *et al.* Human TOB, an antiproliferative transcription factor, is a poly(A)-binding protein-dependent positive regulator of cytoplasmic mRNA deadenylation. *Mol Cell Biol* 2007; **27**: 7791–7801.

17 Funakoshi Y, Doi Y, Hosoda N, Uchida N, Osawa M, Shimada I *et al.* Mechanism of mRNA deadenylation: evidence for a molecular interplay between translation termination factor eRF3 and mRNA deadenylases. *Genes Dev* 2007; **21**: 3135–3148.
18 Ruan L, Osawa M, Hosoda N, Imai S, Machiyama A, Katada T *et al.* Quantitative characterization of Tob interactions provides the thermodynamic basis for translation termination-coupled deadenylase regulation. *J Biol Chem* 2010; **285**: 27624–27631.
19 Hosoda N, Funakoshi Y, Hirasawa M, Yamagishi R, Asano Y, Miyagawa R *et al.* Anti-proliferative protein Tob negatively regulates CPEB3 target by recruiting Caf1 deadenylase. *EMBO J* 2011; **30**: 1311–1323.
20 Jin M, Wang XM, Tu Y, Zhang XH, Gao X, Guo N *et al.* The negative cell cycle regulator, Tob (transducer of ErbB-2), is a multifunctional protein involved in hippocampus-dependent learning and memory. *Neuroscience* 2005; **131**: 647–659.
21 Wang XM, Gao X, Zhang XH, Tu YY, Jin ML, Zhao GP *et al.* The negative cell cycle regulator, Tob (transducer of ErbB-2), is involved in motor skill learning. *Biochem Biophys Res Commun* 2006; **340**: 1023–1027.
22 Maekawa M, Nishida E, Tanoue T.. Identification of the Anti-proliferative protein Tob as a MAPK substrate. *J Biol Chem* 2002; **277**: 37783–37787.
23 Suzuki T, K-Tsuzuku J, Ajima R, Nakamura T, Yoshida Y, Yamamoto T. Phosphorylation of three regulatory serines of Tob by Erk1 and Erk2 is required for Ras-mediated cell proliferation and transformation. *Genes Dev* 2002; **16**: 1356–1370.
24 Ellis RE, Kimble J. The fog-3 gene and regulation of cell fate in the germ line of *Caenorhabditis elegans*. *Genetics* 1995; **139**: 561–577.
25 Xiong B, Rui Y, Zhang M, Shi K, Jia S, Tian T *et al.* Tob1 controls dorsal development of zebrafish embryos by antagonizing maternal beta-catenin transcriptional activity. *Dev Cell* 2006; **11**: 225–238.
26 Yoshida Y, Tanaka S, Umemori H, Minowa O, Usui M, Ikematsu N *et al.* Negative regulation of BMP/Smad signaling by Tob in osteoblasts. *Cell* 2000; **103**: 1085–1097.
27 Tzachanis D, Freeman GJ, Hirano N, van Puijenbroek AA, Delfs MW, Berezovskaya A *et al.* Tob is a negative regulator of activation that is expressed in anergic and quiescent T cells. *Nat Immunol* 2011; **2**: 1174–1182.
28 Groisman I, Ivshina M, Marin V, Kennedy NJ, Davis RJ, Richter JD. Control of cellular senescence by CPEB. *Genes Dev* 2006; **20**: 2701–2712.
29 Ren YG, Martinez J, Virtanen A. Identification of the active site of poly(A)-specific ribonuclease by site-directed mutagenesis and Fe(2+)-mediated cleavage. *J Biol Chem* 2002; **277**: 5982–5987.
30 Dean M, Levine RA, Ran W, Kindy MS, Sonenshein GE, Campisi J. Regulation of c-myc transcription and mRNA abundance by serum growth factors and cell contact. *J Biol Chem* 1986; **261**: 9161–9166.
31 Burns DM, Richter JD. CPEB regulation of human cellular senescence, energy metabolism, and p53 mRNA translation. *Genes Dev* 2008; **22**: 3449–3460.
32 Wu L, Wells D, Tay J, Mendis D, Abbott MA, Barnitt A *et al.* CPEB-mediated cytoplasmic polyadenylation and the regulation of experience-dependent translation of alpha-CaMKII mRNA at synapses. *Neuron* 1998; **21**: 1129–1139.
33 Zearfoss NR, Alarcon JM, Trifilieff P, Kandel E, Richter JD. A molecular circuit composed of CPEB-1 and c-Jun controls growth hormone-mediated synaptic plasticity in the mouse hippocampus. *J Neurosci* 2008; **28**: 8502–8509.
34 Belloc E, Mendez R. A deadenylation negative feedback mechanism governs meiotic metaphase arrest. *Nature* 2008; **452**: 1017–1021.
35 Arumugam K, Wang Y, Hardy LL, MacNicol MC, MacNicol AM. Enforcing temporal control of maternal mRNA translation during oocyte cell-cycle progression. *EMBO J* 2010; **29**: 387–97.
36 Pique M, Lopez JM, Foissac S, Guigo R, Mendez R. A combinatorial code for CPE-mediated translational control. *Cell* 2008; **132**: 434–448.
37 Wang YY, Charlesworth A, Byrd SM, Gregerson R, MacNicol MC, MacNicol AM. A novel mRNA 3′ untranslated region translational control sequence regulates *Xenopus* Wee1 mRNA translation. *Dev Biol* 2008; **317**: 454–466.
38 MacNicol MC, MacNicol AM. Developmental timing of mRNA translation—integration of distinct regulatory elements. *Mol Reprod Dev* 2010; **77**: 662–669.
39 Mateyak MK, Obaya AJ, Sedivy JM. c-Myc regulates cyclin D-Cdk4 and -Cdk6 activity but affects cell cycle progression at multiple independent points. *Mol Cell Biol* 1999; **19**: 4672–4683.
40 Blanchard JM, Piechaczyk M, Dani C, Chambard JC, Franchi A, Pouyssegur J *et al.* C-myc gene is transcribed at high rate in G0-arrested fibroblasts and is post-transcriptionally regulated in response to growth factors. *Nature* 1985; **317**: 443–445.
41 Kindy MS, Sonenshein GE. Regulation of oncogene expression in cultured aortic smooth muscle cells. Post-transcriptional control of c-myc mRNA. *J Biol Chem* 1986; **261**: 12865–12868.
42 Kerkhoff E, Houben R, Loffler S, Troppmair J, Lee JE, Rapp UR. Regulation of c-myc expression by Ras/Raf signalling. *Oncogene* 1998; **16**: 211–216.
43 Kim KC, Oh WJ, Ko KH, Shin CY, Wells DG. Cyclin B1 expression regulated by cytoplasmic polyadenylation element binding protein in astrocytes. *J Neurosci* 2011; **31**: 12118–12128.
44 Novoa I, Gallego J, Ferreira PG, Mendez R. Mitotic cell-cycle progression is regulated by CPEB1 and CPEB4-dependent translational control. *Nat Cell Biol* 2010; **12**: 447–456.
45 Aslam A, Mittal S, Koch F, Andrau JC, Winkler GS. The Ccr4-NOT deadenylase subunits CNOT7 and CNOT8 have overlapping roles and modulate cell proliferation. *Mol Biol Cell* 2009; **20**: 3840–3850.
46 Horiuchi M, Takeuchi K, Noda N, Muroya N, Suzuki T, Nakamura T *et al.* Structural basis for the antiproliferative activity of the Tob–hCaf1 complex. *J Biol Chem* 2009; **284**: 13244–13255.
47 Groisman I, Jung MY, Sarkissian M, Cao Q, Richter JD. Translational control of the embryonic cell cycle. *Cell* 2002; **109**: 473–483.

Supplementary Information accompanies the paper on the Oncogene website (http://www.nature.com/onc)

RNA:

The Hbs1-Dom34 Protein Complex Functions in Non-stop mRNA Decay in Mammalian Cells

Syuhei Saito, Nao Hosoda and Shin-ichi Hoshino

J. Biol. Chem. 2013, 288:17832-17843.
doi: 10.1074/jbc.M112.448977 originally published online May 10, 2013

THE JOURNAL OF BIOLOGICAL CHEMISTRY VOL. 288, NO. 24, pp. 17832–17843, June 14, 2013

The Hbs1-Dom34 Protein Complex Functions in Non-stop mRNA Decay in Mammalian Cells*[S]

Received for publication, December 26, 2012, and in revised form, May 7, 2013 Published, JBC Papers in Press, May 10, 2013, DOI 10.1074/jbc.M112.448977

Syuhei Saito[1], **Nao Hosoda**[1], **and Shin-ichi Hoshino**[2]

From the [‡]*Department of Biological Chemistry, Graduate School of Pharmaceutical Sciences, Nagoya City University, Nagoya 467-8603, Japan*

Background: The non-stop decay (NSD) mechanism has remained undetermined in mammalian cells.
Results: Degradation of unstable non-stop mRNA requires Hbs1, Dom34, and the exosome-Ski complex in mammalian cells.
Conclusion: The NSD mechanism exists in mammalian cells and involves a member of the eRF3 family of G proteins, Hbs1.
Significance: Our work provides a foundation for dissecting the detailed molecular basis of the human NSD mechanism.

In yeast, aberrant mRNAs lacking in-frame termination codons are recognized and degraded by the non-stop decay (NSD) pathway. The recognition of non-stop mRNAs involves a member of the eRF3 family of GTP-binding proteins, Ski7. Ski7 is thought to bind the ribosome stalled at the 3′-end of the mRNA poly(A) tail and recruit the exosome to degrade the aberrant message. However, Ski7 is not found in mammalian cells, and even the presence of the NSD mechanism itself has remained enigmatic. Here, we show that unstable non-stop mRNA is degraded in a translation-dependent manner in mammalian cells. The decay requires another eRF3 family member (Hbs1), its binding partner Dom34, and components of the exosome-Ski complex (Ski2/Mtr4 and Dis3). Hbs1-Dom34 binds to form a complex with the exosome-Ski complex. Also, the elimination of aberrant proteins produced from non-stop transcripts requires the RING finger protein listerin. These findings demonstrate that the NSD mechanism exists in mammalian cells and involves Hbs1, Dom34, and the exosome-Ski complex.

mRNA decay is intimately linked to and regulated by translation. In recent years, it has become clear that members of the eRF3 (eukaryotic translation release factor 3) family of GTP-binding proteins act as signal transducers that couple translation to mRNA decay and play pivotal roles in the regulation of gene expression and mRNA quality control in eukaryotes. Members of this family are structurally characterized by a C-terminal elongation factor 1α-like GTP-binding domain and an N-terminal unique domain (1–4). The C-terminal domain is highly conserved among the members in eukaryotes, whereas the N-terminal domain is less conserved and unique to each family member. The most well studied member, eRF3, is a class II release factor, which brings the class I factor eRF1 into the ribosomal A site containing a termination codon (UAA, UGA, or UAG) and accelerates the peptidyl hydrolase activity of the ribosome (5–7). Involvement of eRF3 in the regulation of mRNA decay was first documented for nonsense-mediated mRNA decay (8), which eliminates mRNA with a premature termination codon (9). After nonsense-containing mRNA is transported to the cytoplasm, the translation termination complex eRF1-eRF3 binds to the ribosome that has arrived at the premature termination codon. The premature termination codon is thought to be recognized as aberrant either by inefficient translation termination caused by the faux UTR (10) or by downstream decay-accelerating elements, including the exon-exon junction complex (11–14). Depending on the species, distinct and/or unified mechanisms are proposed for nonsense-mediated mRNA decay (15–18).

eRF3 is also involved in the regulation of decay of normal mRNA. eRF3 forms a complex with a cytoplasmic poly(A)-binding protein and regulates the deadenylation of general mRNA in both yeast and mammals (19–21). We have proposed that the translation termination complex eRF1-eRF3 binds to poly(A)-binding protein competitively with the deadenylases, and release of the termination complex after translation ends triggers the association of the deadenylases with poly(A)-bound poly(A)-binding protein and accelerates deadenylation of the mRNA (21).

In contrast to the mRNAs with termination codons, mRNAs that lack in-frame termination codons are recognized and degraded by a mechanism called non-stop decay (NSD)[3] (22–24). This system involves another eRF3 family member, Ski7, and the auxiliary Ski complex composed of the DE*x*H RNA helicase Ski2, the tricopeptide repeat protein Ski3, and the WD repeat protein Ski8 (25). NSD also requires the exosome, which consists of nine core proteins, including Rrp40 and the catalytic protein Rrp44 (26). Ski7 associates with the cytoplasmic form of the exosome and the Ski complex through its N-terminal domain (3). Because termination codons are missing in the message, the ribosome continues to translate the 3′-UTR and even the poly(A) tail. In a proposed model, Ski7 binds to the

* This work was supported by Grant-in-aid for Scientific Research on Innovative Areas "RNA Regulation" 20112005 from the Ministry of Education, Culture, Sports, Science and Technology of Japan and Grant-in-aid for Scientific Research (B) 21370080 from the Japan Society for the Promotion of Science (to S. H.).
[S] This article contains supplemental Tables 1 and 2.
[1] Both authors contributed equally to this work.
[2] To whom correspondence should be addressed: Dept. of Biological Chemistry, Graduate School of Pharmaceutical Sciences, Nagoya City University, 3-1 Tanabe-dori, Mizuho-ku, Nagoya 467-8603, Japan. Fax: 8-52-836-3427; E-mail: hoshino@phar.nagoya-cu.ac.jp.

[3] The abbreviations used are: NSD, non-stop decay; FBG, FLAG-β-globin; IRE, iron-responsive element; EGFP, enhanced GFP.

ribosome stalled at the 3′-end of the mRNA and recruits the exosome to trigger fast 3′-to-5′ exonucleolytic degradation of the message. Thus, NSD is translation-dependent (23), but in contrast to normal decay, NSD is not dependent on deadenylation (22). Also, NSD does not require nonsense-mediated mRNA decay factors, including Upf1 (23). The components involved in the yeast NSD mechanism are conserved in mammals except for the key regulator Ski7.

In contrast, mRNAs with a structural propensity to cause ribosome stalling are degraded by no-go decay (27–29). In this mechanism, Hbs1 (the closest relative of eRF3) in complex with the eRF1 homolog Dom34 functions as a regulator (4). As is the case for eRF1-eRF3, the Hbs1-Dom34 complex binds to the A site of the ribosome that is stalled during translation elongation in a codon-nonspecific manner and triggers endonucleolytic cleavage by an unknown nuclease to eliminate the aberrant message (27, 30–33). Recent findings demonstrated that Hbs1-Dom34 also functions as a codon-nonspecific translation termination factor to release peptidyl-tRNA and to accelerate recycling of the stalled ribosome (34, 35).

These mRNA decay mechanisms are believed to be conserved among eukaryotes with the exception of NSD. Ski7 is found only in a subset of saccharomycete yeast cells but not in mammalian cells, and even the presence of the NSD mechanism itself has remained largely enigmatic. In contrast, there are reports supporting the presence of NSD in mammalian cells. First, Frischmeyer *et al.* (23) have shown that a non-stop β-glucuronidase reporter mRNA was low at steady state in HeLa cells. Second, α-globin non-stop mRNA was reported to be unstable in MEL and HeLa cells (24). In contrast, there are published data refuting the existence of NSD in mammals. A study using a GFP-based reporter in HeLa cells showed that the steady-state amount of non-stop mRNA was not significantly reduced relative to the wild-type message, and no significant difference was observed between the stability of the wild-type and non-stop mRNAs (36). Moreover, even in clinical cases, inconsistent results have been reported. In Diamond-Blackfan anemia, mutant RPS19 (ribosomal protein S19) mRNA lacking a stop codon was low compared with wild-type mRNA from a healthy donor (37). Similar results were reported for other clinical cases (38). In contrast, in a mitochondrial neurogastrointestinal encephalopathy patient, mutant (non-stop) TYMP mRNA was stable and coexisted with wild-type mRNA at similar levels (39).

Here, we examined the existence of NSD in mammals in detail based on the following five criteria: (i) stability of non-stop mRNA, (ii) dependence on translation, (iii) requirement for eRF3 family GTP-binding protein, (iv) requirement for the exosome-Ski complex, and (v) complex formation between the eRF3 family G protein and the exosome. We demonstrate that NSD actually exists in mammalian cells and involves Hbs1-Dom34 in complex with the exosome-Ski complex.

EXPERIMENTAL PROCEDURES

Plasmids—pFBG control (with the in-frame stop codon in the β-globin 3′-UTR mutated) was constructed by inverse PCR using pFLAG-CMV5/TO-β-globin (21) and the primer pair NH0193/NH0194. pFBG non-stop was generated by inverse PCR using pFBG control and NH0195/NH0004. To construct p5FBG control and p5FBG non-stop, the β-globin gene was amplified by PCR using either pFBG control or pFBG non-stop and the primer pair NH0047/NH0048 and inserted into the HindIII and EcoRV sites of pCMV-5×FLAG (40) to yield pCMV-5×FLAG-β-globin control or pCMV-5×FLAG-β-globin non-stop, respectively. The 5×FLAG-tagged β-globin gene was then amplified by PCR using either pCMV-5×FLAG-β-globin control or pCMV-5×FLAG-β-globin non-stop and the primer pair NH0618/NH0048 and inserted into the EcoRV and PstI sites of pFLAG-CMV5/TO (21). pIRE-FBG non-stop was generated by inverse PCR using pFBG non-stop and the primer pair NH0670/NH0671. pT7-TR, which expresses the T7-tagged tetracycline receptor, was generated by inverse PCR using pcDNA6/TR (Invitrogen) and the primer pair NH0383/NH0389. To construct pFLAG-Hbs1, cDNA encoding Hbs1 was amplified by PCR using petmRFS (2) and the primer pair NH0273/NH0414 and inserted into the EcoRI and XhoI sites of pCMV-FLAG (21). To construct pFLAG-Dom34, cDNA encoding Dom34 was amplified by RT-PCR using cDNA reverse-transcribed from HeLa cell total RNA as a template and the primer pair NH0275/NH0276 and inserted into the EcoRI site of pCMV-FLAG. To construct p5×Myc-Ski2, cDNA encoding Ski2 was amplified by PCR using the primer pair NH0237/NH0238 and the BC015758 clone (Open Biosystems) as a template and inserted into the EcoRI and XhoI sites of pCMV-5×Myc (41). To construct p5×Myc-Dis3, cDNA encoding Dis3 was amplified by PCR using the primer pair NH0089/NH0090 and the KIAA1008 clone as a template and inserted into the SalI and BglII sites of pCMV-5×Myc. Either pEGFP-C1 (Clontech) or p5×FLAG-EGFP (41) was used as a transfection/loading control. Primer sequences are listed in supplemental Table 1.

Cell Culture and DNA/RNA Transfection—HeLa cells were cultured in Dulbecco's modified Eagle's medium (Nissui) supplemented with 5% fetal bovine serum. DNA/RNA transfection was performed using Lipofectamine 2000 (Invitrogen) or polyethylenimine Max (Polysciences, Inc.) according to the manufacturers' instructions.

Northern Analysis and Real-time PCR—HeLa cells were transfected with the specified plasmids and siRNAs using Lipofectamine 2000. Total RNA was isolated and analyzed by Northern blotting as described previously (21, 41). In the transcriptional pulse-chase analysis, HeLa cells were transfected with pT7-TR, p5×FLAG-EGFP, either pFBG control or pFBG non-stop, and the specified siRNAs. 48 h after transfection, the cells were treated with 10 ng/ml tetracycline for 2.5 h to induce transcription, washed twice with phosphate-buffered saline to remove tetracycline completely, and harvested at the specified times after transcriptional shutoff. Total RNA was isolated and analyzed by Northern blotting. The levels of 5FBG, FBG, and 5×FLAG-EGFP mRNAs were quantitated from the Northern blot using Image Gauge Version 4.23 (Fujifilm). Real-time PCR analysis was performed using the StepOne real-time PCR system with *Power* SYBR Green PCR Master Mix (Applied Biosystems). Listerin and Mtr4 mRNAs were amplified using the primer pairs NH0619/NH0620 and NH0730/NH0731, respectively. GAPDH mRNA was amplified as described previously